

1 **Short-term variations of platinum concentrations in contrasting coastal environments:**  
2 **the role of primary producers**

3 Melina Abdou<sup>1, 4\*</sup>, Teba Gil-Díaz<sup>1</sup>, Jörg Schäfer<sup>1</sup>, Charlotte Catrouillet<sup>1</sup>, Cécile Bossy<sup>1</sup>,  
4 Lionel Dutruch<sup>1</sup>, Gérard Blanc<sup>1</sup>, Antonio Cobelo-García<sup>2</sup>, Francesco Massa<sup>3</sup>, Michela  
5 Castellano<sup>3</sup>, Emanuele Magi<sup>3</sup>, Paolo Povero<sup>3</sup>, Mary-Lou Tercier-Waeber<sup>4</sup>

6 <sup>1</sup>*University of Bordeaux, UMR CNRS 5805 EPOC, 33615 Pessac, France,*

7 <sup>2</sup>*Instituto de Investigaci3n Mariñas (IIM-CSIC), Vigo, Galicia, Spain*

8 <sup>3</sup>*University of Genoa, DISTAV-DCCI, 16132 Genoa, Italy*

9 <sup>4</sup>*University of Geneva, Dept. of Inorganic and Analytical Chemistry, 1211 Geneva 4,*  
10 *Switzerland*

11 *\*Corresponding author: melina.abdou@unige.ch*

12 **Abstract**

13 Short-term variations of Pt concentrations and primary production indicators were compared  
14 in three contrasting coastal sites during spring bloom: (i) the Gironde Estuary mouth (SW  
15 France), (ii) the semi-enclosed Arcachon Bay (SW France), and (iii) the urbanized Genoa  
16 Harbor (NW Italy). At each site, surface seawater sampling and physical-chemical  
17 measurements were combined to study diel cycles (over 25 hours) of dissolved Pt  
18 concentrations in seawater (Pt<sub>D</sub>) and master variables reflecting primary production activity  
19 (chlorophyll-a, phaeopigments, and particulate organic carbon, POC concentrations).  
20 Plankton nets were used in all sites, providing for the first time plankton Pt concentrations  
21 (Pt<sub>PK</sub>) over a whole diel cycle (Gironde Estuary mouth) and spot sampling (Arcachon Bay and  
22 Genoa Harbor) in the coastal zone. Bivalves (wild oysters or mussels), reflecting organisms at  
23 higher trophic levels, were also collected at all sites. The POC/Chl-a ratios in the collected  
24 particulate material suggested high contribution of phytoplankton to the particulate matter in  
25 the productive Gironde Estuary mouth. At this site, phytoplankton activity partly controlled Pt  
26 cycling and particle/dissolved Pt partitioning during daytime. During the night, zooplankton  
27 grazing may release Pt into the dissolved phase. These processes are partly masked by  
28 external factors such as tide or local Pt sources, especially in more confined and/or urbanized  
29 coastal water bodies such as the Arcachon Bay and the Genoa Harbor. Platinum levels in  
30 plankton and bivalves from these contrasting sites along the Atlantic and Mediterranean  
31 coasts tended to reflect the general Pt levels in seawater. These results clearly suggest that (i)  
32 Pt contamination of coastal waters and marine organisms has become a common feature in  
33 urbanized sites and (ii) Pt transfer to the marine food chain starts at the basic level of primary  
34 producers. By concentrating Pt (Bioconcentration Factor: BCF ~ 10<sup>4</sup>), phytoplankton may  
35 serve as a biomonitor to assess Pt contamination in coastal environments.

36 **Keywords:** Technology Critical Element, seawater, phytoplankton, bioconcentration

37 **Declarations of interest:** none

38

## 39 **1. Introduction**

40 Platinum (Pt) is a Technology Critical Element (TCE) for which there is an increasing need  
41 for accurate assessment of environmental impacts and natural dynamics (Cobelo-García et al.,  
42 2015). This emerging metallic contaminant belonging to the Platinum Group Elements (PGE)  
43 has been increasingly used in various applications over few decades, including vehicle  
44 catalytic converters and Pt-based anticancer drugs. Such emissions induce a general increase  
45 in Pt concentrations in all Earth compartments, with anthropogenic activities accounting for  
46 more than 80 % of Pt fluxes at the Earth's surface (Sen and Peucker-Ehrenbrink, 2012).  
47 Catalytic converters efficiently reduce gaseous pollutant emissions from car exhaust, but  
48 thermal and mechanical abrasions during vehicle functioning lead to PGE release into the  
49 environment (Artelt et al., 1999; Rauch et al., 2004a). Urban runoff and atmospheric  
50 deposition transport Pt emissions to the aquatic environment and ultimately to the coastal area  
51 and the sea. In addition, anti-cancer chemotherapy has been applying Pt-based compounds for  
52 decades (e.g. Lenz et al., 2007) and surface waters draining both effluents from hospitals with  
53 oncology ward and domestic wastewater receive excretion of Pt-based anticancer drugs from  
54 patients and outpatients at home (Vyas et al., 2014), which may lead to increasing Pt levels in  
55 urban sewage. Consequently, dissolved Pt concentrations in open ocean seawater (Colodner et  
56 al., 1993; Suzuki et al., 2014) or pristine estuaries (Pađan et al., 2019) are generally far below  
57 seawater concentrations near urbanized coastal or estuarine systems (Abdou et al., 2019;  
58 Cobelo-García et al., 2013; Mashio et al., 2017, 2016; Obata et al., 2006). Coastal  
59 environments facing ever-growing human pressure (~ 40 % of world's population live within  
60 100 km of the coast; UN, 2017) therefore receive increasing anthropogenic Pt inputs from  
61 these various sources (Ruchter et al., 2015). Despite the crucial need for accurate assessment  
62 of the extent of Pt contamination and for the understanding of Pt biogeochemical cycles in  
63 coastal systems, so far only very few field studies address this issue.

64 Platinum bioavailability to living organisms and especially to marine biota is non-negligible.  
65 In fact, the limited environmentally relevant information available in the literature include Pt  
66 concentrations in marine macroalgae (Hodge et al., 1986), in marine bivalves (Abdou et al.,  
67 2019, 2016; Neira et al., 2015), and in dolphins (Essumang, 2008). There is even less  
68 information on the possible transfer mechanisms controlling Pt accumulation throughout the

69 aquatic trophic chain. At the base of this marine trophic chain, numerous algal species are  
70 able to sequester considerable amounts of trace elements from the dissolved phase, exerting  
71 a control on trace metal concentrations and cycling in marine systems (González-Dávila,  
72 1995). As decaying and settling particles, phytoplankton cells also represent an important  
73 vehicle for the vertical transport of contaminants in the water column in marine environments  
74 through cell sinking into deeper waters and/or ingestion by consumers in surface waters  
75 (González-Dávila, 1995; Shams et al., 2014). Although phytoplankton communities may play  
76 a key role in the geochemical cycling of trace metals in coastal ecosystems (Caetano and  
77 Vale, 2003; Cloern, 1996), no study has reported yet on Pt concentrations in phytoplankton  
78 and the potential influence of this marine biological compartment on Pt cycling.

79 Based on sampling at ~ 1 h resolution covering diel cycles, as performed for the first time in  
80 the Gironde Estuary mouth, the Arcachon Bay and the Genoa Harbor, this study focuses on Pt  
81 cycles under different hydrological conditions and anthropogenic pressure. The objectives of  
82 the present work are (i) to identify potential relations in short-term (hourly timescale) Pt  
83 concentrations with phytoplankton production/degradation cycles, (ii) to assess the possible  
84 transfer of Pt through the aquatic trophic chain, and (iii) to investigate the potential use of  
85 phytoplankton material as a geochemical tool for biomonitoring Pt contamination in coastal  
86 systems. The outcomes of the present work are a part of the PhD thesis by Abdou (2018).

87

## 88 **2. Material and Methods**

### 89 2.1. Study area and sample collection

#### 90 *Study site characteristics*

91 The Gironde Estuary (~170 km in length; 80,000 km<sup>2</sup> watershed area) is a major European  
92 estuary located in southwest France (Fig. 1A), considered a model system for physical,  
93 hydrological and geochemical studies, especially on trace element transport and reactivity in  
94 anthropogenically-impacted watersheds (Lanceleur et al., 2011). Its most important  
95 hydrodynamic characteristics are the semi-diurnal, meso- to macro-tidal regime, and the  
96 maximum turbidity zone (MTZ; > 1 g.L<sup>-1</sup> of suspended particulate matter), varying seasonally  
97 with river flow and exported occasionally to the Atlantic Ocean (Castaing and Allen, 1981;  
98 Doxaran et al., 2009). The Gironde Estuary drains the urban area of Bordeaux (1,190,000  
99 inhabitants), located ~ 100 km upstream from the estuary mouth. Sampling was performed in  
100 the Gironde Estuary mouth on-board the Research Vessel (R/V) Thalia (TGIR FOF) at a fixed  
101 sampling site (45°40'00.2"N, 1°10'33.0"W, Fig. 1A). This site is located on the western

102 channel lying to the north, with a bottom depth varying between 10 and 30 m and a width  
103 between 2 and 4 km. This channel was artificially created by dredging in 1935 (Allen, 1971).  
104 Sampling took place in June 2017 (22<sup>nd</sup>-23<sup>rd</sup>) during low discharge conditions ( $Q \sim 235 \text{ m}^3 \cdot \text{s}^{-1}$ ,  
105 DIREN, public agency), over 29 hours (18 samples). This sampling period was  
106 characterized by the beginning of spring tide and tidal coefficients from 81 to 92 (tidal  
107 amplitudes varying from 3.80 m to 4.35 m). In addition, wild oyster samples (*Crassostrea*  
108 *gigas*; 15 organisms, ~ 9 cm shell length) were collected at the La Fosse sampling site  
109 (45°28'23.4"N, 0°59'50.9"W; Fig. 1A).

110 The Arcachon Bay is a meso-tidal lagoon in southwest France, ~ 100 km to the south of the  
111 Gironde Estuary mouth (Fig. 1B) and represents an important breeding ecosystem for regional  
112 seafood production, especially oysters. The sampling site (Comprian), located in a main  
113 current channel of the bay, receives inputs from the Leyre River, several cities surrounding  
114 the site (~ 90,000 inhabitants), and seawater from the Atlantic Ocean. In May 2015 (21<sup>st</sup> –  
115 22<sup>nd</sup>), hourly sampling over a diel cycle of 31 hours was performed on board R/V Planula IV  
116 (TGIR FOF) at a fixed sampling site (Comprian site, 44°40.823'N, 1°05.902'W, Fig. 1B). The  
117 end of spring tide characterized our sampling period with tidal coefficients from 89 to 72  
118 (tidal amplitudes varying from 3.10 m to 3.70 m). Wild oysters (*C. gigas*; 10 organisms,  
119 ~ 9 cm shell length) were collected manually on a bank near the Comprian site during low  
120 tide.

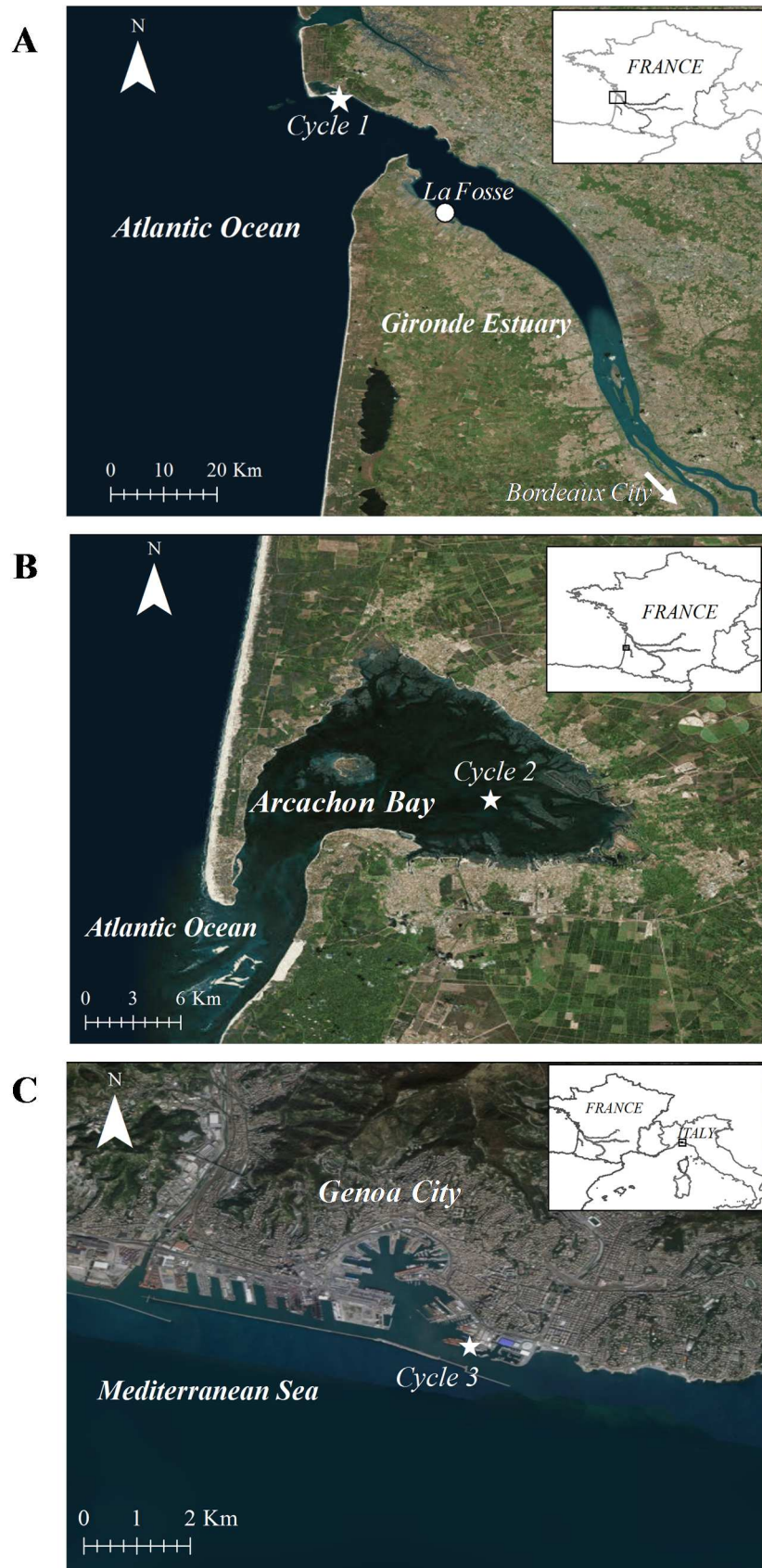
121 The Genoa Harbor is an artificial harbor in the northwest coast of Italy (Ligurian Sea,  
122 Fig. 1C) and one of the most important ports of the Mediterranean Sea. The area is exposed to  
123 anthropogenic pollution originating from sea-based (ferries, shipyards, marinas...) and land-  
124 based activities of the city of Genoa (580,000 inhabitants). The innermost part of the Genoa  
125 Harbor is the Old Port hosting a ferry terminal, several marinas and receiving urban sewage  
126 effluents (Ruggieri et al., 2011). Outside the Old Port a wide, less confined area protected by  
127 artificial breakwaters extends to the east and to the west, hosting diverse industrial activities  
128 and receiving discharges from a coal-fired power plant, treated urban wastewater and  
129 untreated surface run-off (Ruggieri et al., 2011). In April 2016 (19<sup>th</sup> – 20<sup>th</sup>), hourly sampling  
130 covering a diel cycle of 25 hours was performed inside the Genoa Harbor at the CNR  
131 platform (National Research Council, 44°23'44"N, 08°55'53"E, Fig. 1C). At this site, very  
132 small tidal amplitude of ~ 0.2 m was monitored. At the platform, wild mussels (*Mytilus*  
133 *galloprovincialis*, 10 organisms, ~ 7 cm shell length) were also collected manually.

134

135 *Sample collection and processing*

136 At all sites, surface seawater (~ 2 to 5 m depth) was pumped using an electric pumping  
137 system connected to Teflon tubing. Seawater samples for dissolved Pt ( $Pt_D$ ) analysis were  
138 immediately filtered through 0.2  $\mu\text{m}$  polycarbonate filters (Nucleopore®) using a filter-  
139 syringe (Sartorius®) and placed in pre-cleaned 60 mL Teflon FEP bottles (Nalgene®),  
140 previously rinsed with filtrate. Samples were acidified to  $\text{pH} = 1$  (36.5 – 38 % HCl Baker®  
141 Instra) and stored in the dark at 4 °C pending analysis. Suspended Particulate Matter (SPM)  
142 and Particulate Organic Carbon (POC) concentrations in surface water were determined by  
143 filtration of precise water volumes through pre-combusted and pre-weighed filters  
144 (Whatman® GF/F, 0.7  $\mu\text{m}$ ; Etcheber et al., 2007). The filters were rinsed with MilliQ water to  
145 remove salts and were then oven dried to constant weight at 50 °C, weighed again, and kept in  
146 the dark at room temperature pending analysis. Furthermore, particulate samples were  
147 collected for determination of chlorophyll-a and phaeopigments by filtering seawater  
148 (Whatman® GF/F, 0.7  $\mu\text{m}$ ) and deep-freezing the filters (- 80 °C) pending analysis. For  
149 qualitative and quantitative analyses of phytoplankton, seawater samples were fixed with 2 %  
150 seawater-buffered formalin solution and kept in the dark at 4 °C pending analysis.

151 Material for plankton Pt ( $Pt_{PK}$ ) analysis was collected, every 1 to 2 hours, by surface  
152 horizontal (~ 1m depth) sampling at the fix sampling station during the diel cycle of the  
153 Gironde Estuary. In the other sites, plankton material was collected at variable times during  
154 daytime in the Arcachon Bay (n = 3; Comprian station) and the Genoa Harbor (n = 5). Given  
155 the strong tidal currents and the related suspension of silts and fine-grained sand in the  
156 Gironde Estuary, we used sampling nets with nominal cut-off of 200  $\mu\text{m}$  for the Gironde  
157 Estuary mouth; whereas the cut-off for the other sampling sites was 20  $\mu\text{m}$ . Seawater  
158 containing concentrated plankton cells was retrieved from the collector and centrifuged at  
159 1,500 rpm. The supernatant was removed and the collected residue was deep-frozen, freeze-  
160 dried, and kept in the dark at room temperature pending analysis.



161  
 162 Fig. 1: Study areas with sampling sites (white stars). A: Gironde Estuary (Cycle 1), B: Arcachon Bay  
 163 (Cycle 2), C: Genoa Harbor (Cycle 3). Wild bivalve samples were collected at La Fosse (oysters)  
 164 in the Gironde Estuary and at the “cycle” sampling sites for the Arcachon Bay (Comprian; oysters)  
 165 and the Genoa Harbor (mussels).

166 After manual collection of wild bivalves, organisms were cleaned and depurated under  
167 oxygenation by bubbling air in seawater during 48 hours. The organisms were dissected and  
168 soft tissues were placed in acid-cleaned polypropylene (PP) tubes (DigiTUBEs, SCP  
169 SCIENCE®). Samples were then deep-frozen, freeze dried, grinded in an agate mortar and  
170 kept in the dark at room temperature pending analysis.

171 At all sites, physical-chemical parameters including temperature, salinity, and O<sub>2</sub> saturation  
172 level (O<sub>2</sub>%) were measured *in situ* with a portable TetraCon 96® probe (PROFILINE,  
173 WTW), and pH with a Sentix 41® probe (PROFILINE, WTW). On site, average bottom  
174 depth of the Gironde Estuary was of ~ 14 m, while it was of ~ 5 m for both the Arcachon Bay  
175 and the Genoa Harbor. Information on solar radiation (irradiance) was obtained from the  
176 “Meteo France” and “Infoclimat” databases for the SW of France and from “DICCA”  
177 (Dipartimento di Ingegneria Civile, Chimica e Ambientale, University of Genoa) for the  
178 Genoa Harbor. We retrieved tidal information from the website maree.info and  
179 mareografico.it; and river discharges in the Gironde Estuary from the National Hydrographic  
180 Databank (DIREN).

181

## 182 2.2. Analytical methods

### 183 *Platinum in seawater*

184 The total dissolved Pt concentration in the filtered seawater samples was analyzed by  
185 Adsorptive Cathodic Stripping Voltammetry (AdCSV) as described in Cobelo-García et al.  
186 (2014b). Measurements were carried out using a µAutolab Type III potentiostat (Metrohm®)  
187 connected to a polarographic stand (Metrohm® 663 VA stand) equipped with three  
188 electrodes: (i) a hanging mercury drop electrode (HMDE, the working electrode), (ii) a  
189 silver/silver-chloride (Ag/AgCl) as reference electrode, and (iii) a glassy carbon auxiliary  
190 electrode. A polytetrafluoroethylene (PTFE) voltammetric cell was used in all experiments  
191 and the potentiostat was controlled using the NOVA 2.1 software. Elimination of organic  
192 matter by UV oxidation was performed by placing sample aliquots in capped Teflon FEP  
193 tubes with overnight irradiation using two 64 W UV lamps (NIQ 60/35 XL, Heraeus) under a  
194 fume hood. Aliquots (10 mL) of UV-digested sample were pipetted into the voltammetric cell  
195 together with 30 µL of 3.3 mM formaldehyde (37–41 % Analytical Reagent Grade, Fisher  
196 Chemical®), and 30 µL of 0.45 mM hydrazine sulfate (Analytical Reagent Grade, Fisher  
197 Chemical®). Platinum concentrations were quantified by the standard addition method,  
198 adding a controlled amount of a Pt stock solution prepared daily from a mono-elementary Pt

199 standard solution (1000  $\mu\text{g}\cdot\text{mL}^{-1}$  PLASMACAL, SCP Science®). We applied a deposition  
200 time of 300 s and experimental parameters described elsewhere (Cobelo-García et al., 2014b).

201 The detection limit for  $\text{Pt}_D$  measured by AdCSV (calculated as 3 x blank standard deviation,  
202  $n = 20$ ) was estimated to  $0.15 \text{ pmol}\cdot\text{L}^{-1}$ . In the absence of Certified Reference Material  
203 (CRM) for dissolved Pt in seawater, analytical quality of the voltammetric procedure was  
204 evaluated by determination of Pt spiked CRM seawater (CASS-6, NRCC) giving recoveries  
205  $> 80\%$  and precision expressed as Relative Standard Deviation (RSD) of  $\sim 15 \%$  ( $n = 3$ ) at the  
206  $2.5 \text{ pmol}\cdot\text{L}^{-1}$  range.

#### 207 *Platinum in biological samples: plankton material and bivalves*

208 Ashing was applied as a pre-concentration method for Pt content in biological material (e.g.  
209 Schäfer et al., 1998). Dry plankton or bivalve material ( $\sim 1 \text{ g}$ ) was weighed and ashed in acid-  
210 cleaned porcelain crucibles at  $800 \text{ }^\circ\text{C}$  during 3 hours according to the heating scheme  
211 described by Nygren et al. (1990). Ashed samples were weighed again to determine the  
212 organic matter percentage (loss on ignition, L.O.I. technique) and samples were then  
213 transferred into PP tubes, and digested at  $110 \text{ }^\circ\text{C}$  for 3 hours with 2 mL HCl and 1 mL  $\text{HNO}_3$   
214 (30 % HCl and 65 %  $\text{HNO}_3$  Suprapur, Merck®) as described in Abdou et al. (2018). Cooled  
215 digestates were then diluted in 10 mL MilliQ® water and centrifuged at 4000 rpm for 10 min  
216 ( $20 \text{ }^\circ\text{C}$ ). The supernatant was stored in acid-cleaned PP tubes at  $4 \text{ }^\circ\text{C}$  in the dark pending  
217 analysis.

218 Platinum concentrations in plankton material ( $\text{Pt}_{PK}$ ) or bivalves ( $\text{Pt}_{BV}$ ) were determined by  
219 Triple Quadrupole-Inductively Coupled Plasma Mass Spectrometry (TQ-ICP-MS, Thermo®  
220 iCAP TQ), using standard addition method, as described previously for AdCSV. Hafnium-  
221 oxide ions ( $\text{HfO}^+$ ) interfere with all Pt isotopes making Pt accurate quantification by ICP-MS  
222 difficult in environmental samples (Djingova et al., 2003). Platinum concentrations in natural  
223 biological samples were measured by ICP-MS after mathematical correction of the  $\text{HfO}^+$   
224 interference using  $^{194}\text{Pt} / ^{195}\text{Pt}$  natural ratio (assuming that  $\text{HfO}^+$  is the dominant spectral  
225 interference on those selected isotopes; Abdou et al., 2018). The detection limit for Pt levels  
226 in biota measured by TQ-ICP-MS (calculated as 3 x blank standard deviation,  $n = 10$ ) was  
227 estimated to  $0.15 \text{ pmol}\cdot\text{g}^{-1}$  for a nominal ashed sample mass of 50 mg and  $0.005 \text{ pmol}\cdot\text{g}^{-1}$  for  
228 typical biological sample mass of 1.5 g.

229 Since no CRM for Pt in biological matrices is available, aliquots of plankton net material  
230 were analyzed in parallel using both ICP-MS and AdCSV, i.e. two independent measurement  
231 techniques. They provided, as observed for bivalve samples in a previous study (Abdou et al.,  
232 2018), similar results between both methods (RSD  $\sim 15 \%$ ,  $n = 5$ ). Quality control was also



233 performed using available CRMs for Pt concentrations in solid matrices: Jsd-2 sedimentary  
234 rocks (indicative value from Geological Survey of Japan) and BCR®-723 road dust (IRMM).  
235 Analyses of Jsd-2 and BCR®-723 gave satisfactory results with precision of ~ 15 % and  
236 respective recovery values of 65% and > 80 % (n = 3) applying the same interference  
237 corrections as for biological samples.

#### 238 *Phytoplankton analysis*

239 Phytoplankton assemblages in water were identified in four samples of the Gironde cycle  
240 (three samples collected during daytime on the first day at 8 am, 2 pm and 7 pm and one  
241 sample retrieved during the night of the second day at 1 am), in the Arcachon Bay (diel cycle  
242 in May 2017; eight samples) and the Genoa Harbor (three samples). In all cases, fixed  
243 phytoplankton cells were counted according to the Utermöhl method (Utermöhl, 1958). This  
244 technique applies the combined use of an inverted-microscope and a special counting  
245 chamber, where phytoplankton has been gathered through a sedimentation cylinder (Hasle,  
246 1978). This method allows for the identification of the main taxa of autotrophic  
247 microplankton (in particular species of diatoms, dinoflagellates –mainly armored) and  
248 coccolithophorids. However, this method is not recommended for other flagellates that may  
249 possibly be damaged during the fixation process nor for pico-nanoplankton, due to the very  
250 small dimensions of the cells (Zingone et al. 2010).

#### 251 *Chlorophyll-a, phaeopigments, and POC*

252 Chlorophyll a (Chl-a) was extracted in 90 % acetone and determined by spectrofluorometry  
253 (Trilogy, Turner, Strickland and Parsons, 1972). Dilutions of a solution of Chl-a (*Anacystis*  
254 *nidulans*, 1 mg.L<sup>-1</sup>; C-6144; Sigma-Aldrich®) was used to calibrate the fluorimeter.  
255 Phaeopigments (phaeo) were also determined using the same analysis (after acidification, HCl  
256 3M). Detection limit of the technique was 0.1 µg.L<sup>-1</sup> while precision was ~ 15 %. Due to  
257 sampling logistics, Chl-a and phaeo data in the Genoa Harbor are only available for daytime  
258 period. Particulate Organic Carbon (POC) was analyzed with a LECO® CS-125 after  
259 carbonate elimination with 2M HCl as described elsewhere (Etcheber et al., 2007). Analytical  
260 quality was checked by measuring CRMs (e.g. LECO 501–503). Accuracy was within 5 % of  
261 the certified values and the analytical error generally < 5 % (% RSD).

262

263 2.3. Data treatment

264 *Bioconcentration factors*

265 Bioconcentration factors (BCF; Arnot and Gobas, 2006) were determined according to the  
266 following Equation 1:

267 
$$\text{BCF} = \frac{\text{Pt}_{\text{biota}}}{\text{Pt}_{\text{D}}} \times 10^3 \quad (1)$$

268 With  $\text{Pt}_{\text{biota}}$ : the Pt concentration in biota sample (corresponding to  $\text{Pt}_{\text{PK}}$  or  $\text{Pt}_{\text{BV}}$  in this study),  
269  $\text{Pt}_{\text{D}}$ : the dissolved Pt concentration, and  $10^3$  a correcting factor for units.

270 *Particulate organic matter content*

271 Plankton material collected with nets may contain lithogenic material such as mineral(-oxide)  
272 particles (e.g. silicates, iron(Fe)-oxides etc...), as well as non-living organic aggregates and  
273 phytodetritus. Accordingly, the attribution of Pt content in the samples to phytoplankton  
274 material alone may be wrong, implying the need to account for abiotic particles and non-  
275 living organic matter that may complex Pt ions as other trace metals (Twining et al., 2011).  
276 Existing field studies often analyze bulk particulate matter under conditions where authors  
277 can assume low lithogenic and detrital contributions for a range of trace metals (Twining and  
278 Baines, 2013 and references therein). In order to evaluate the proportion of organic material in  
279 our samples, we used the loss on ignition technique (*Section 2.2*) providing the percentage of  
280 organic matter present in the particulate material (Particulate Organic Matter: POM) from  
281 plankton nets. We also evaluated POC/SPM ratio (POC%) in order to have the proportion of  
282 organic material in the SPM collected on filters (0.7  $\mu\text{m}$  mesh size). Results from those two  
283 methods are shown in the Supporting Information (SI). Finally, we determined the POC/Chl-a  
284 ratio (filters 0.7  $\mu\text{m}$  mesh size) in order to evaluate qualitatively the contribution of living  
285 phytoplankton to the organic material (Savoie et al., 2003).

## 286 **3. Results**

### 287 3.1. Physical-chemical parameter variations

#### 288 *Gironde Estuary*

289 Tide height variations are presented in Fig. 2A. Master physical-chemical parameters  
290 monitored over the Cycle 1 (Fig. 2B) showed variations of SPM concentration from ~ 5 to  
291 60 mg.L<sup>-1</sup>. Two maximum values occurred the first day at 10 am and during the night  
292 (> 40 mg.L<sup>-1</sup>). The pH and salinity measurements followed the same trend with variations  
293 from 8.06 to 8.20 and from 30 to 32.5, respectively (Fig. 2B). Those parameters were related  
294 to tidal regimes with higher salinity, pH and lower SPM concentrations at high tide. Solar  
295 radiation varied from 0 to 300 J.cm<sup>-2</sup>, showing two maxima (at 11:30 am on the first day and  
296 at 1 pm on the second day; Fig. 2C). Oxygen saturation levels varying from ~ 100 to 110 %  
297 coincided with high tide at 5 pm on the first day (Fig. 2C). During the night, O<sub>2</sub>% levels are at  
298 their minimum, coinciding with low salinity. In the middle of the nighttime, O<sub>2</sub>% increased  
299 only slightly, fully displaying the second O<sub>2</sub>% maximum during the second day at 11:30 am  
300 during low tide. Temperature values varied between 19.2 and 20.2 °C (Fig. 2C). Lower  
301 temperatures partly co-occurred with highest salinity (especially on the second day) and  
302 slightly higher values were monitored during the second day (11:30 am). Chlorophyll-a values  
303 ranged between ~ 4 and 8 µg.L<sup>-1</sup> while phaeopigments varied between ~ 2 and 10 µg.L<sup>-1</sup>  
304 (Fig. 2D). Chlorophyll-a concentrations showed an overall decreasing trend from the  
305 beginning of sampling until 7 am on the second day though increasing and reaching a  
306 maximum at 11:30 am. Phaeopigments seemed to follow SPM concentrations and showed a  
307 maximum at 11:30 am alike Chl-a levels. Calculated POC/Chl-a ratio variations showed  
308 values between ~ 50 and 300 (Fig. 2D).

#### 309 *Arcachon Bay*

310 Results from Cycle 2 (Arcachon Bay) showed tide-related physical-chemical parameters  
311 (Fig. 3A, B, and C). The pH measurements follow the salinity trend oscillating at high and  
312 low tide, between 8.02 and 7.84 and between 32 and 22, respectively (maxima at 9 pm and  
313 9 am; Fig. 3B). In general, SPM concentrations ranged from ~ 10 to 50 mg.L<sup>-1</sup> and followed  
314 tidal dynamics. Oxygen saturation levels varied from 75 to 85 % (i.e., always below the 100%  
315 saturation observed in the Gironde Estuary mouth; Fig. 3C). Temperature showed opposite  
316 variations (between 15.2 °C and 17.5 °C; Fig. 3C). Solar radiation reached maximum values  
317 (~ 300 J.cm<sup>-2</sup>) at 2 pm on the first day and 1 pm on the following day (Fig. 3C).

318 Chlorophyll-a concentrations showed little variations between  $\sim 1$  and  $3.5 \mu\text{g.L}^{-1}$  while  
319 phaeopigments varied from  $\sim 0.5$  to  $3.5 \mu\text{g.L}^{-1}$  (Fig. 3D). Lower values of Chl-a occurred  
320 during nighttime compared to daytime concentrations. Pigment levels seemed to co-vary with  
321 POC/Chl-a ratio (ranging from 200 to 700; Fig. 3D) and with SPM concentrations.

### 322 *Genoa Harbor*

323 Results from the CNR Platform in the Genoa Harbor were very different from those in the  
324 previous sites. Salinity was constantly at  $\sim 37.2$  as no tidal variation of similar amplitude  
325 occurred at this site (Fig. 4A and B). The pH values were also constant and close to  $\sim 8.3$   
326 while SPM concentrations varied little from  $\sim 2$  to  $8 \text{mg.L}^{-1}$  (i.e. 6-fold lower than in the  
327 Atlantic sites; Fig. 4B). Oxygen saturation levels ( $\text{O}_2\%$ ) were between 96 % and 100 %, i.e.  
328 between those observed in the Gironde Estuary mouth (minimum 100%) and in the Arcachon  
329 Bay, showing higher values during the day (Fig.4 C). Temperature variations seemed to  
330 follow a similar trend with values between  $16.3^\circ\text{C}$  and  $17.4^\circ\text{C}$ . Solar radiation varied from 0  
331 to  $350 \text{J.cm}^{-2}$  with a maximum occurring at 11 am (Fig.4 C).

332 Pigment concentrations showed increasing trends during the second day with values ranging  
333 between  $\sim 0.8$  and  $1.4 \mu\text{g.L}^{-1}$  and  $0.4$  and  $0.5 \mu\text{g.L}^{-1}$  for Chl-a and phaeopigments,  
334 respectively (Fig. 4D). The POC/Chl-a ratio was nearly constant with average values of  $\sim 130$   
335 (Fig. 4D).

336

## 337 3.2. Phytoplankton composition

### 338 *Gironde Estuary*

339 Microscope observations showed phytoplankton abundance varying between  $\sim 36,000$  and  
340  $58,000 \text{cells.L}^{-1}$ . Average percentages for daytime (three samples) showed  $\sim 80\%$  contribution  
341 of Bacillariophyceae, mostly represented by *Pseudonitzschia spp.*, *Chaetoceros spp.*,  
342 *Asterionellopsis spp.*, and *Odontella spp.* Dinophyceae composed  $\sim 10\%$  of the phytoplankton  
343 (*Ceratium fusus* and armoured dinoflagellates) and the last 10% was Prymnesiophyceae.  
344 Samples collected at 2 pm and 7 pm featured the association between the Bacillariophyceae  
345 *Thalassiosira sp.* and the coccolithophorid *Reticulofenestra sessilis*. During nighttime (one  
346 sample), slightly higher proportion of Bacillariophyceae occurred ( $\sim 85\%$ ), while  
347 Prymnesiophyceae became more abundant over Dinophyceae (15% against 2%, respectively).  
348 This phytoplankton composition was characteristic of this study site (REPHY, 2019).

349 *Arcachon Bay*

350 Phytoplankton composition was studied in water samples collected in Compiègne in spring  
351 2017. The abundance varied between ~ 19,000 and 40,000 cells.L<sup>-1</sup>. Results showed that as  
352 for the Gironde Estuary, Bacillariophyceae was the main class represented in the  
353 phytoplankton assemblage (83.6-96.5 % over the cycle), despite showing a shift in the  
354 dominant class with tidal variations. At this site, long-term monitoring data and previous  
355 studies confirmed that in spring this class represented ~ 80% of the total phytoplankton  
356 abundances and were mainly composed during high tide of *Leptocylindrus danicus*,  
357 *Pseudonitzschia* spp., *Chaetoceros* spp., *Dactyliosolen fragilissimus* and *Asterionella*  
358 *glacialis* (REPHY, 2019; Ifremer/ODE/LITTORAL/LERAR, 2017; Glé et al., 2007).

359 *Genoa Harbor*

360 During the Genoa Harbor diel cycle, abundance of phytoplankton cells varied between  
361 ~ 60,000 and 167,000 cells.L<sup>-1</sup>. Bacillariophyceae were as well the most abundant taxonomic  
362 group (80-98.2 %). This group was mainly composed of *Chaetoceros* spp., *Leptocylindrus*  
363 spp., *Pseudonitzschia* spp., *Thalassiosira* spp., or *Lauderia* spp. Another field campaign in  
364 spring 2017 also confirmed the dominance of Bacillariophyceae during diel cycle (72.0-  
365 97.5 %). This composition is typical for the season in the coastal Gulf of Genoa (Carli et al.,  
366 1994).

367

368 3.3. Platinum concentrations in seawater and plankton material

369 *Gironde Estuary*

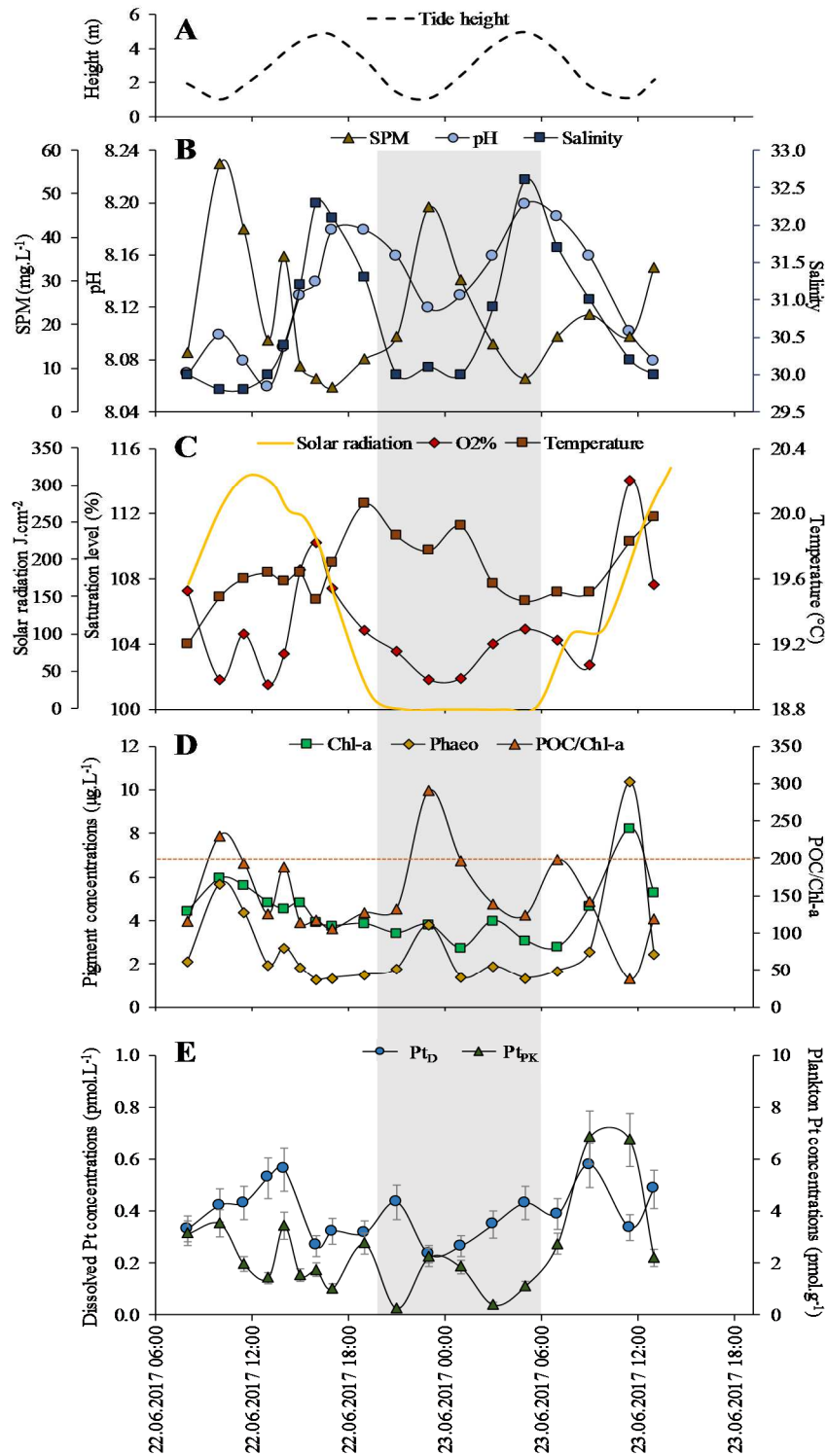
370 Hourly measured Pt<sub>D</sub> concentrations ranged from 0.23 to 0.58 pmol.L<sup>-1</sup> showing alternating  
371 trends (Fig. 2E). Three main peaks occurred: (i) one on the first day at 2 pm (0.56 pmol.L<sup>-1</sup>),  
372 followed by a decrease down to 0.27 pmol.L<sup>-1</sup>, (ii) a small peak close to the night at 9 pm, and  
373 (iii) a third peak of 0.58 pmol.L<sup>-1</sup> at 9 am on the second day. During the Cycle 1, Pt<sub>PK</sub>  
374 concentrations ranged from 0.27 to 6.84 pmol.g<sup>-1</sup> (Fig. 2E). Visual examination of plankton  
375 net material suggested that samples were mainly composed of phytoplankton during the day  
376 and zooplankton during the night. Plankton Pt concentrations displayed a generally decreasing  
377 trend on the first day from 8 am to 9 pm. During the nighttime, minimum values occurred in  
378 between two slight increases at 11 pm and 1 am. The following day, Pt<sub>PK</sub> showed increasing  
379 levels from the early morning to maxima of ~ 7 pmol.g<sup>-1</sup> at 9 am and 11:30 am.

380 *Arcachon Bay*

381 Dissolved  $Pt_D$  concentrations varied from 0.25 to 0.75  $\text{pmol.L}^{-1}$  (Fig. 3E) on the first day and  
382 during nighttime. In the morning of the second day (from 8 am onwards),  $Pt_D$  levels tended to  
383 increase towards a high tide maximum at ~ 11 am and thereafter showed a clear decrease  
384 towards minimum values at 6 pm. The  $Pt_{PK}$  concentrations monitored at the Comprian site  
385 varied between 8.65 and 16.49  $\text{pmol.g}^{-1}$  (Fig. 3E).

386 *Genoa Harbor*

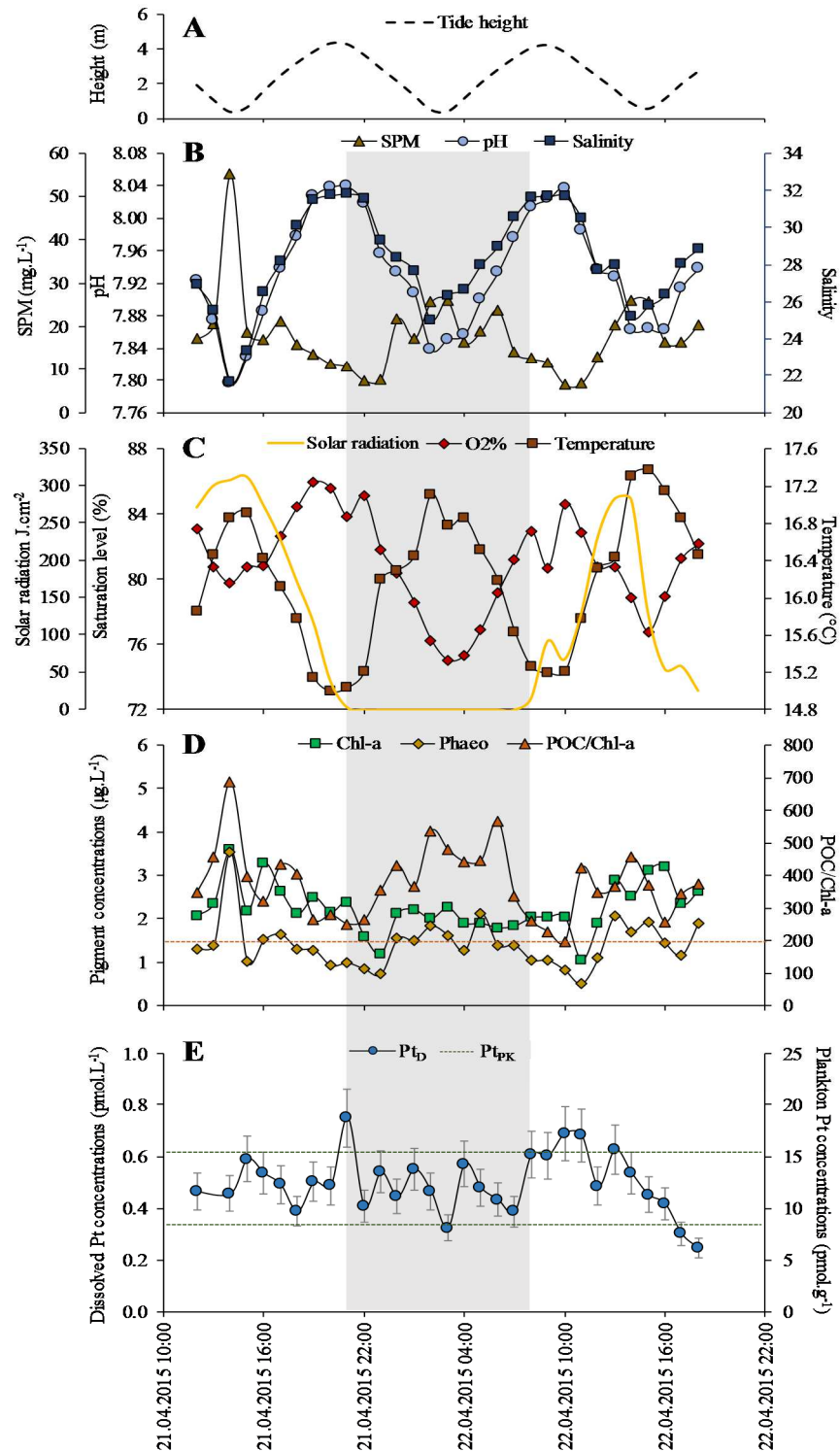
387 No clear trend occurred for  $Pt_D$  concentrations (variations between 0.37  $\text{pmol.L}^{-1}$  and  
388 0.83  $\text{pmol.L}^{-1}$ ), although a general decreasing trend seemed to occur on the second day  
389 between 9 am and 8 pm (Fig. 4E). Nighttime  $Pt_D$  concentrations showed minimal values. The  
390  $Pt_{PK}$  levels measured at this site varied between 15 and 34  $\text{pmol.g}^{-1}$  (Fig. 4E).



391

392 Fig. 2: Short-term variations in physical-chemical variables, algal pigments and Pt concentrations in  
 393 seawater and plankton material from the Gironde Estuary in June 2017. A: Tide height (m, dashed  
 394 line) B: Suspended Particulate Matter (SPM,  $\text{mg.L}^{-1}$ , triangles), pH (circles), and Salinity (squares); C:  
 395 Solar radiation ( $\text{J.cm}^{-2}$ , solid line), Dissolved oxygen saturation levels ( $\text{O}_2\%$ , diamonds), and  
 396 Temperature ( $^{\circ}\text{C}$ , squares); D: Chlorophyll-a (Chl-a,  $\mu\text{g.L}^{-1}$ , squares), Phaeopigments (Phaeo,  $\mu\text{g.L}^{-1}$ ,  
 397 diamonds), and Particulate Organic Carbon / Chlorophyll-a ratio (POC/Chl-a, triangles), the dashed  
 398 line represents the limit for dominance of living phytoplankton in POM (Savoye et al., 2003); E:  
 399 Dissolved Pt concentrations (pmol.L<sup>-1</sup>) and Plankton Pt concentrations (pmol.g<sup>-1</sup>)

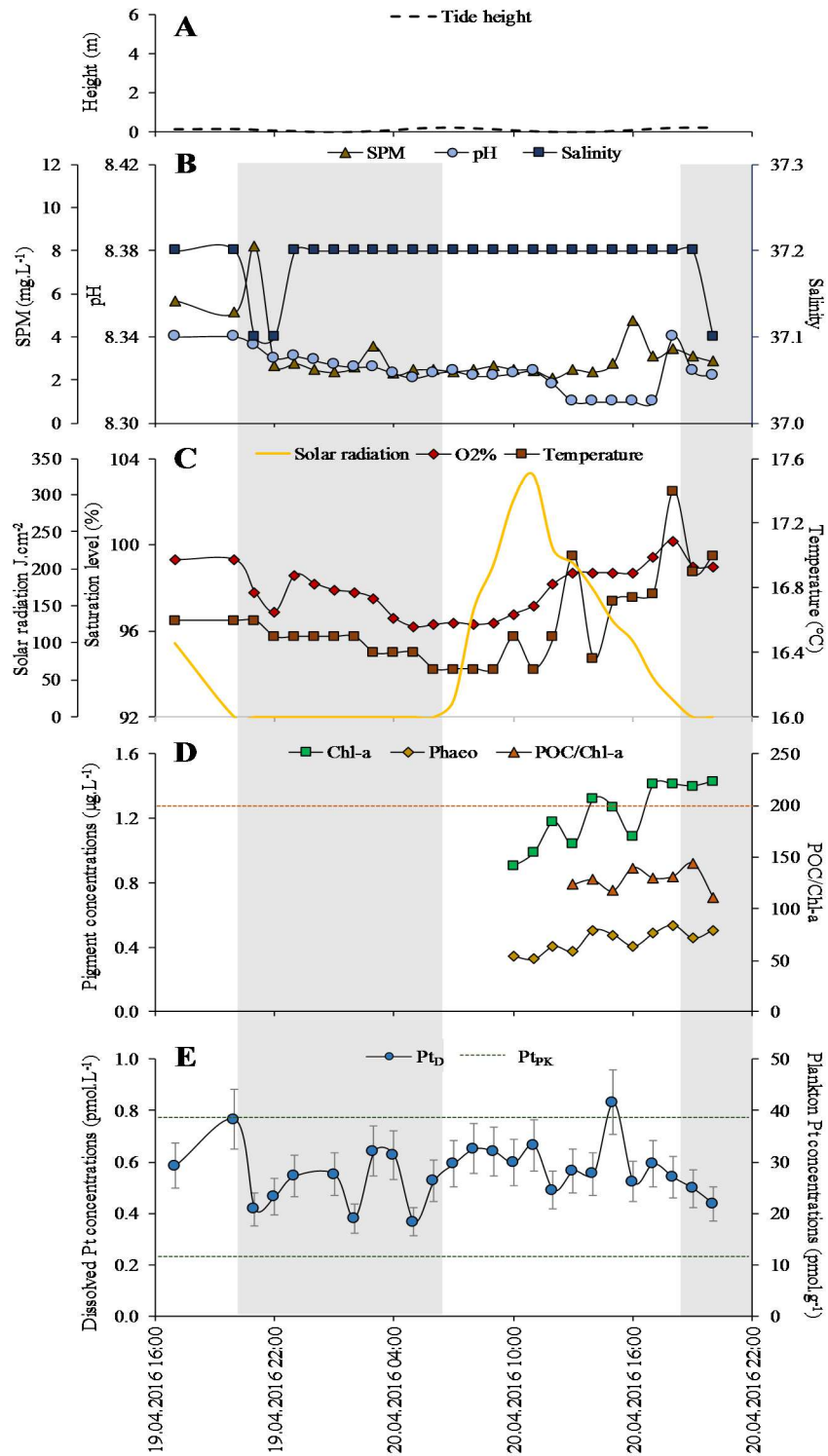
400 pmol.L<sup>-1</sup>, circles), and plankton Pt (Pt<sub>PK</sub>, pmol.g<sup>-1</sup>, triangles) concentrations. The gray strip represents  
 401 nighttime (Abdou, 2018).



402  
 403 Fig. 3: Short-term variations in physical-chemical variables, algal pigments and Pt concentrations in  
 404 seawater and plankton material from the Arcachon Bay in April 2015. A: Tide height (m, dashed line);  
 405 B: Suspended Particulate Matter (SPM, mg.L<sup>-1</sup>, triangles), pH (circles), and Salinity (squares); C:  
 406 Solar radiation (J.cm<sup>-2</sup>, solid line), Dissolved oxygen saturation levels (O<sub>2</sub>%, diamonds), and  
 407 Temperature (°C, squares); D: Chlorophyll-a (Chl-a, µg.L<sup>-1</sup>, squares), Phaeopigments (Phaeo, µg.L<sup>-1</sup>,  
 408 diamonds), and Particulate Organic Carbon / Chlorophyll-a ratio (POC/Chl-a, triangles), the dashed



409 line represents the limit for dominance of living phytoplankton in POM (Savoye et al., 2003); E:  
410 Dissolved Pt (Pt<sub>D</sub>,  
411 pmol.L<sup>-1</sup>, circles) and range of plankton Pt (Pt<sub>PK</sub>, pmol.g<sup>-1</sup>, dashed line) concentrations. The gray strip  
412 represents nighttime (Abdou, 2018).



413

414 Fig. 4: Short-term variations in physical-chemical variables, algal pigments and Pt concentrations in  
 415 seawater and plankton material from the Genoa Harbor in April 2016. A: Tide height (m, dashed line);  
 416 B: Suspended Particulate Matter (SPM,  $\text{mg.L}^{-1}$ , triangles), pH (circles), and Salinity (squares); C:  
 417 Solar radiation ( $\text{J.cm}^{-2}$ , solid line), Dissolved oxygen saturation levels ( $\text{O}_2\%$ , diamonds), and  
 418 Temperature ( $^{\circ}\text{C}$ , squares); D: Chlorophyll-a (Chl-a,  $\mu\text{g.L}^{-1}$ , squares), Phaeopigments (Phaeo,  $\mu\text{g.L}^{-1}$ ,  
 419 diamonds), and Particulate Organic Carbon / Chlorophyll-a ratio (POC/Chl-a, triangles), the dashed  
 420 line represents the limit for dominance of living phytoplankton in POM (Savoye et al., 2003); E:  
 421 Dissolved Pt concentrations (pmol.L<sup>-1</sup>, circles) and Pt<sub>4x</sub> (dotted line) (Pt<sub>D</sub>,

422 pmol.L<sup>-1</sup>, circles) and range of plankton Pt (Pt<sub>PK</sub>, pmol.g<sup>-1</sup>, dashed line) concentrations. The gray strip  
423 represents nighttime (Abdou, 2018).

424 3.4. Platinum concentrations and bioconcentration factors in plankton and bivalves  
 425 from the three contrasting sites

426 Table 1 shows average  $Pt_D$  concentrations for the three sites with values of 0.38, 0.48, and  
 427 0.56  $\text{pmol.L}^{-1}$  for the Gironde, the Arcachon Bay, and the Genoa Harbor, respectively. In  
 428 order to compare  $Pt_{PK}$  in plankton material from the three sites, we report only daytime  
 429 average  $Pt_{PK}$  concentrations of the Gironde Estuary mouth. At this site,  $Pt_{PK}$  was 3.01  $\text{pmol.g}^{-1}$   
 430 <sup>1</sup>, while in the Arcachon Bay and the Genoa Harbor,  $Pt_{PK}$  were clearly higher, i.e.  $\sim 12$  and  
 431 24  $\text{pmol.g}^{-1}$ , respectively (Table 1).

432 Platinum concentrations in bivalves ( $Pt_{BV}$ ) were 1.69  $\text{pmol.g}^{-1}$  in wild oysters (*C. gigas*) from  
 433 the La Fosse site, i.e. slightly greater than in the Arcachon Bay (1.01  $\text{pmol.g}^{-1}$ ; Table 1). Wild  
 434 mussels (*M. galloprovincialis*) from the Genoa Harbor showed  $Pt_{BV}$  of 2.44  $\text{pmol.g}^{-1}$ .

435 The resulting BCF (Equation 1) for plankton ( $BCF_{PK}$ ) ranged from  $7.75 \times 10^3$  to  $4.23 \times 10^4$  at  
 436 the different sites, whereas BCF for bivalves ( $BCF_{BV}$ ) varied from  $2.09 \times 10^3$  to  $2.27 \times 10^4$ .

437 Table 1: Platinum concentrations in seawater ( $Pt_D$ ;  $\text{pmol.L}^{-1}$ ), plankton ( $Pt_{PK}$ ;  $\text{pmol.g}^{-1}$ ) and bivalves  
 438 ( $Pt_{BV}$ ;  $\text{pmol.g}^{-1}$ ) from three study sites, and the associated bioconcentration factors (BCF, calculated  
 439 from Equation (1);  $BCF_{PK}$  and  $BCF_{BV}$ ; Abdou, 2018).

Sampling site	$[Pt]_D$ ( $\text{pmol.L}^{-1}$ )			$[Pt]_{PK}$ ( $\text{pmol.g}^{-1}$ )			$[Pt]_{BV}$ ( $\text{pmol.g}^{-1}$ )			$BCF_{PK}$ ( $\times 10^3$ )	$BCF_{BV}$ ( $\times 10^3$ )
	Mean	SD	n	Mean	SD	n	Mean	SD	n		
<b>Gironde Estuary</b>	0.38	0.15	18	3.01	1.78	13	1.69	0.15	5	7.75	22.73
<b>Arcachon Bay</b>	0.48	0.11	30	11.76	3.40	3	1.01	0.28	10	24.43	2.09
<b>Genoa Harbor</b>	0.56	0.11	25	23.77	9.48	5	2.44	0.69	10	42.30	4.35

440

## 441 4. Discussion

### 442 4.1. Tidal regimes and Pt concentrations in three contrasting sites

#### 443 *Gironde Estuary*

444 Platinum concentrations in estuaries can both derive from natural sources including rock  
445 leaching and weathering (Upper Continental Crust Pt content of  $2.6 \text{ pmol.g}^{-1}$ ; Rudnick and  
446 Gao, 2003); and from anthropogenic sources that include industrial activities, sewage  
447 effluents or Pt-bearing particles emitted by car catalytic converters. In this study, Pt  
448 concentrations were monitored at the very external part of the Gironde Estuary mouth under  
449 low discharge conditions ( $Q \sim 235 \text{ m}^3.\text{s}^{-1}$ ). Average  $\text{Pt}_{\text{D}}$  levels of this northeastern Atlantic  
450 Ocean coastal site ( $0.38 \pm 0.15 \text{ pmol.L}^{-1}$ ) confirm previous North Atlantic Ocean  $\text{Pt}_{\text{D}}$  values  
451 ( $\sim 0.1 - 0.3 \text{ pmol.L}^{-1}$ , Colodner, 1991; López-Sánchez et al. 2019). Variations of  $\text{Pt}_{\text{D}}$  from  
452  $0.33 \text{ pmol.L}^{-1}$  to  $0.58 \text{ pmol.L}^{-1}$  over the cycle may be partly due to mixing of estuarine waters  
453 with ocean water. The range of  $\text{Pt}_{\text{D}}$  values were in line with  $\text{Pt}_{\text{D}}$  addition along the Gironde  
454 Estuary salinity gradient as reported for similar discharge conditions ( $Q \sim 410 \text{ m}^3.\text{s}^{-1}$   
455 following a 3 month period with  $Q \sim 240 \text{ m}^3.\text{s}^{-1}$ ), resulting in  $\text{Pt}_{\text{D}}$  of  $0.41 \text{ pmol.L}^{-1}$  at salinity  
456 of 28.1 (Cobelo-García et al., 2014a).

457 The limited available information on Pt speciation in seawater suggests that Pt(IV) under the  
458 form  $\text{PtCl}_5(\text{OH})^{2-}$  dominates, while Pt(II) as the species  $\text{Pt}(\text{OH})_2$  dominates in freshwater  
459 (Cobelo-García et al., 2014a, 2013; Gammons, 1996; Pađan et al., 2019). Estuarine particle-  
460 water interactions along the salinity gradient are likely controlled by electrostatic interactions  
461 between SPM surface and inorganic aqueous species (Cobelo-Garcia et al., 2008; Cobelo-  
462 García et al., 2014a). Accordingly, elevated  $\text{Pt}_{\text{D}}$  concentrations with increasing salinity (Pt  
463 desorption from SPM) were studied in the Krka Estuary (Pađan et al., 2019) and partially  
464 observed along the Gironde salinity gradient (Cobelo-García et al., 2014a). The present  
465 Cycle 1 site being located at a very external part of the estuary mouth, with rather low SPM  
466 concentrations compared to the inner estuary, the variations of Pt concentrations do not  
467 clearly reflect such processes despite potential influence of SPM tidal variations.

468 The small amplitude in salinity values  $\sim 30$  and  $32.5$  (Fig. 2B) recorded the tidal regime and  
469 the influence of freshwater expulsion during ebb tide (Fig. 2A). High tide occurred at 5 pm  
470 the first day and 5 am on day two, fitting salinity and pH measurements (Fig. 2A and B).  
471 Under these conditions, waters were generally colder and more oxygenated compared to low  
472 tide conditions. However, those parameters also featured correlations with day/night cycle as  
473 well as pigment concentrations (Fig. 2D and C; see *Section 4.2.*). Suspended Particulate

474 Matter (SPM) concentrations generally followed tidal regime with higher levels reached at  
475 low tides (10 am, 11 pm, and 1 pm; Fig. 2A and B). Considering that the majority of Pt  
476 contamination in the estuary may originate from continental sources, such as urban-impacted  
477 riverine inputs (e.g. Ruchter et al., 2015), one would expect higher Pt levels co-occurring with  
478 low tide events. Cobelo-García et al. (2014a) found that inside the Gironde Estuary, Pt<sub>D</sub> levels  
479 may reach 0.84 pmol.L<sup>-1</sup> in the low salinity range (S = 5.4) suggesting that this system is not  
480 extensively contaminated by Pt but still represents a net source of Pt<sub>D</sub> to the coastal ocean.  
481 This idea is in line with the present observations for Pt<sub>D</sub> levels during daytime (Fig. 2E)  
482 suggesting an increase of Pt<sub>D</sub> concentrations on the first day from 8 am to 2 pm together with  
483 ebb tide, while on the second day the last measurement seemed to feature a new increase. One  
484 would need more data to confirm the influence of riverine pollution, also considering that  
485 during nighttime Pt<sub>D</sub> levels are at the lowest under low tide conditions.

486 Plankton Pt concentration profile suggested no direct correlation with tidal regimes (Fig. 2E)  
487 but seemed to relate to day/night cycle as discussed in *Section 4.2*. However, some exceptions  
488 occurred during the sampling cycle. During the fortnightly cycle of varying tidal ranges,  
489 important changes in sediment resuspension and transport may take place. Accordingly,  
490 during neap to spring phase, tidal ranges vary from 1.5 m to 5.5 m at the estuary mouth  
491 together with increasing current velocity (Castaing and Allen, 1981; Sottolichio and Castaing,  
492 1999). Our sampling campaign was carried out at the initiation of spring tide (average tidal  
493 range of 4 m; Fig. 2A) with tidal coefficients of 81 on the first day and 92 on the second  
494 (maximum salinity value higher during the second day, Fig. 2B). Under these conditions and  
495 resulting currents, large-scale sediment resuspension may take place with increased sediment  
496 concentrations in surface water (Castaing and Allen, 1981) especially at mid-tide. This is  
497 partly visible from increasing SPM concentrations on the first day at 2 pm at mid-flow tide  
498 (Fig. 2A and B). At the same time, slightly higher phaeopigment concentrations occurred  
499 together with higher POC/Chl-a ratio (Fig. 2D). In fact, in shallow systems or in deeper sites  
500 close to the shore, benthic POM may contribute to the POM pool of surface water through  
501 resuspension of microphytobenthos or decaying macrophytes (Irigoién and Castel, 1997;  
502 Liénart et al., 2017). These phytobenthic layers are potential metal carriers and their tidal  
503 suspension may influence metal cycles in coastal systems (Strady et al., 2011). Slight  
504 increases in Pt<sub>PK</sub> levels on the first day at 2 pm and 7 pm may result from such processes.  
505 Although no SPM concentrations increase occurred at 7 pm on day one, microscopic  
506 observations of those samples revealed the association of *Reticulofenestra sessilis* with  
507 *Thalassiosira sp.*, which is a typical association of deep photic layers (e.g. Frada et al., 2010)  
508 with *Thalassiosira sp.* representing more than 15% of the total diatoms. Those findings

509 therefore support the hypothesis of increasing concentrations of particulate Pt related to  
510 phytobenthos transport in surface seawater under energetic tidal conditions.

#### 511 *Arcachon Bay*

512 The position of the sampling site in the Arcachon Bay (Comprian Channel) allowed for more  
513 amplitude in the salinity variations and more influence of freshwater inputs (salinity range  
514 from 22 to 32; Fig. 3B). The pH variations followed the tidal regime as well as SPM  
515 concentrations with more turbid waters at low tide and a range of values similar to those of  
516 the Gironde Estuary. This field campaign also took place during spring tide with tidal  
517 coefficient of  $\sim 100$ . Contrary to the Gironde Estuary cycle, temperature co-varied strictly  
518 with the tidal regimes, rather than with solar radiation (Fig. 3A and C). Tide, and solar  
519 radiation/primary production to a lesser extent, seemed to control O<sub>2</sub> saturation level, since  
520 relatively higher O<sub>2</sub> saturation minima occurred during the day than during the night under  
521 low tide conditions (Fig. 3A and C). At this site, pigment concentrations were positively  
522 correlated with SPM concentrations suggesting that Chl-a and phaeopigments were tide-  
523 related with higher concentrations at low tide (Fig.3A, B and D).

524 Comprian sampling site, in this semi-enclosed bay, is located closer to urban/industrial  
525 activities (Arcachon agglomeration) than the Gironde Estuary mouth. This suggests  
526 potentially greater influences of Pt inputs from the surrounding urban areas, including surface  
527 run off and sewage from the urban agglomerations around the Arcachon Bay. Despite no  
528 significant differences between Pt<sub>D</sub> levels in the two sites, such urban sources existing in the  
529 Arcachon Bay may explain the slightly higher average value recorded for Pt<sub>D</sub> concentrations  
530 compared to the Gironde Estuary mouth ( $0.48 \pm 0.11 \text{ pmol.L}^{-1}$  and  $0.38 \pm 0.15 \text{ pmol.g}^{-1}$ ,  
531 respectively; Table 1). The major part of sewage discharge (draining hospital effluents and  
532 domestic wastewaters) from Arcachon City itself and the closest surroundings takes place into  
533 the open ocean at  $\sim 40$  km to the south of the Bay inlet. One cannot exclude that such sewage  
534 release may partly move back towards the bay with coastal waters which might contribute to  
535 the highest Pt<sub>D</sub> levels occurring at high tide at 9 pm on the first day and 11 am on the second  
536 one (Fig. 3E). Nevertheless, the monitored Pt<sub>D</sub> profile did not show a clear tidal cycle.  
537 Potential sediment resuspension and microphytobentic sources may also be important factors  
538 in this shallow site under energetic tidal conditions as supported by the fact that at this site the  
539 contribution of benthic POM may account for  $\sim 20\%$  (Liéart et al., 2017).

#### 540 *Genoa Harbor*

541 The Genoa Harbor featured very different conditions since no tidal regimes similar to the  
542 previous sites occurred. Tide is generally less than 30 cm inside the harbor (Capello et al.,

2016). This explains the constant salinity of 37.2 and pH values of 8.3 (Fig. 4B). Moreover, sampling took place at ~ 5 m depth that is below the main influence of freshwater torrents (Capello et al., 2016) and no rainfall occurred during the sampling month. Our salinity records therefore mainly reflect seawater influence. However, freshwater inputs from both natural torrents such as the Bisagno River or other urban/industrial discharges take place in the harbor area (e.g. Ruggieri et al., 2011). Small variations in salinity values could be related to temporary freshwater inputs occurring twice at the beginning of the nighttime (9 pm on the first day and 8 pm on the second). However, similar to the Arcachon Bay, in the semi-enclosed Genoa Harbor, no clear trends in  $Pt_D$  occurred (Fig. 4E). This suggests, that the observed variations probably reflect changing inputs and biogeochemical recycling of anthropogenic Pt in this heavily urbanized and industrialized harbor. Dissolved Pt levels during daytime ( $0.60 \pm 0.08 \text{ pmol.L}^{-1}$ ) were generally higher than  $0.42 \pm 0.01 \text{ pmol.L}^{-1}$ , i.e. the typical value of the open Mediterranean Sea surface water (Ligurian Current; Abdou et al., 2019). Lowest  $Pt_D$  concentrations occurred during the night, which may support a decrease in Pt inputs related to daily human activities. Platinum sources including urban sewage typically show greater values during the day due to excretion of anticancer drugs (Kümmerer and Helmers, 1997) both from oncologic inpatients in hospitals and from outpatients at home (Lenz et al., 2007; Vyas et al., 2014). A great contribution can also derive from urban heavy traffic roads, including a major highway surrounding the harbor area. Automobile catalyst emissions are an important source of Pt to urban aquatic systems (Rauch et al., 2004a). Considering potential short-range atmospheric deposition (López-Sánchez et al., 2019), traffic-related Pt source may be considerably reduced during the nighttime. Other Pt sources include industrial effluents and emissions that are present in the harbor area (e.g. coal and oil industries; Finkelman and Aruscavage, 1981; Peavy, 1958).

567

#### 568 4.2. Platinum cycles and primary production

The attribution of Pt concentrations to phytoplankton implies the identification of the composition of the collected particulate material. Literature reports POC/Chl-a ratios in the range of 20 to 200 for estuarine phytoplankton-dominated POM in estuary mouths during summer-fall (Cifuentes et al., 1988; Savoye et al., 2003). Especially, ratios of  $80 \pm 20$  are typical of newly produced, living phytoplankton (Savoye et al., 2012). Ratios higher than 200 could result from detrital or degraded POM that dominates in the upper estuary. Other authors differentiate POC/Chl-a ratios lower than 200 for autotrophic and higher than 200 for mixo/heterotrophic organisms or detrital matter predominance (Bentaleb et al., 1998).



578 Previous studies conducted in the Gironde Estuary report that limited phytoplankton primary  
579 production is possible in this turbid estuary with pigment levels probably explained by inputs  
580 of riverine or seaward phytoplankton (David et al., 2005; Irigoien and Castel, 1997).  
581 However, primary production and associated phytoplankton uptake of trace metals occur  
582 upstream from the MTZ (e.g. Cu; Petit et al., 2013). The present study site is located in a  
583 more external part of the Gironde Estuary mouth where intense primary production occurred.  
584 In fact, relatively high Chl-a levels (daytime average of  $5 \mu\text{g.L}^{-1}$ ) support productivity  
585 occurring at the estuary mouth together with POC % (daytime average 4 %; Table S1, SI)  
586 being clearly higher than in the inner, more turbid part of the estuary (1.5 % in the MTZ  
587 without seasonal variation; Etcheber et al., 2007). Low levels of POC/Chl-a ratios i.e. below  
588 200, suggested a dominance of living phytoplankton in POM (Fig. 2D; Savoye et al., 2003).  
589 These conditions go along with a general oxygen oversaturation of the water mass (lowest  $\text{O}_2$   
590 saturation levels of  $> 100 \%$ ). These values were generally in phase with temperature, with  
591 increasing values during daytime and low levels during nighttime. Similar daily variations  
592 were already reported in the Gironde Estuary mouth (Baudrimont et al., 2005). The  
593 combination of summer conditions including high irradiance and low river discharge  
594 ( $Q \sim 235 \text{ m}^3.\text{s}^{-1}$ , upstream position of the MTZ) might therefore play a role in the  
595 development of phytoplankton cells. During this cycle, POC/Chl-a ratios followed the SPM  
596 concentration variations, with higher value at high tide and decreasing values during the flow  
597 until the beginning of the second day. Relatively high ratios exceeding 200 during ebb tide on  
598 the first day might be related to the transport of detrital material in freshwater. Similar  
599 phaeopigment variations, which are representative of degraded cells, support this hypothesis.

600 Chlorophyll-a followed SPM variations to a certain extent but more generally showed a  
601 decreasing trend during the first day and the night. The fact that Chl-a variations do not match  
602 tidal regimes may be explained by an on-site production of algal cells (autochthonous  
603 phytoplankton) rather than a transport of phytoplankton to the estuary mouth (allochthonous  
604 phytoplankton). Accordingly, out of the MTZ, increasing light penetration in the water  
605 column allows for autochthonous phytoplankton addition to POM (Savoye et al., 2012).  
606 Primary production may be light-driven rather than nutrient-limited, as Chl-a concentrations  
607 co-vary with irradiance during the daytime, which is in accordance with predictions on light-  
608 limited phytoplankton growth (Goosen et al., 1999; Irigoien and Castel, 1997). However, in  
609 the Gironde Estuary mouth, the general decreasing trend of Chl-a concentrations could still be  
610 related to nutrient depletion and to a potentially declining phase of phytoplankton bloom  
611 (Platt et al., 1992). Considering primary production relationship with light, on the first day

612 limitation may occur owing to relatively high SPM concentrations that could reduce light  
613 penetration in the water column (Castelle et al., 2009) and therefore photosynthetic processes.  
614 During the first day and nighttime, the decreasing trend of Chl-a concentrations suggests that  
615 no intensive, continuous autochthonous primary production took place, after the highest levels  
616 of the day reached at 10 am under maximal solar radiation.

617 Decreasing trend in Chl-a concentrations co-varied with similar, generally decreasing  $Pt_{PK}$   
618 concentrations. At the same time, increasing trends occurred for  $Pt_D$  variations inducing a  
619 clear shift in Pt partitioning. Various biogeochemical processes in coastal waters (e.g.  
620 desorption, adsorption, dissolution/precipitation, bio- uptake or release) may transfer metals  
621 between the dissolved and the particulate phases (e.g. Turner, 2007). Decaying phytoplankton  
622 cells associated with Pt may lead to decreasing  $Pt_{PK}$  concentrations through cell lysis and/or  
623 vertical cell sinking. Although exact transfer mechanisms explaining exchanges of Pt between  
624 different carrier phases are widely unknown, the observed variations in  $Pt_D$  and  $Pt_{PK}$  may be  
625 either due to (i) internal transfer processes or (ii) external source/sinks releasing or  
626 sequestering  $Pt_D$  from the estuarine water column. Internal transfer processes imply  
627 equilibrated mass balance, whereas non-equilibrated mass balances would suggest an open  
628 system involving external sources or sinks. Since no information was available on algal cell  
629 abundance in our plankton material, we did not perform mass balance calculations nor assess  
630 internal transfer. External transfer through cell sinking may also explain differences observed  
631 between  $Pt_{PK}$  decrease and  $Pt_D$  variations. Biogenic particles can sink more or less rapidly  
632 (depending on algal species; e.g. Luoma et al., 1998) and oscillate in the water column due to  
633 sediment resuspension cycles, especially in high-energy systems such as the Gironde Estuary.  
634 Accordingly, physical mechanisms may mask biogeochemical exchanges of Pt between the  
635 dissolved and the particulate phases by (i) sequestering Pt-bearing particles in sediments or  
636 (ii) releasing  $Pt_{PK}$  and/or  $Pt_D$  from temporary sinks/sources including micro-phytobenthos  
637 mats and increasing  $Pt_{PK}$  levels as discussed in *Section 4.1*.

638 During the night and low tide, decreasing Chl-a levels suggest, together with low salinity, that  
639 in the downward part of the estuarine maximum turbidity zone degradation of phytoplankton  
640 occurs. Chlorophyll-a being degraded faster than the whole POM, increasing POC/Chl-a  
641 levels arose during phytoplankton degradation (Cifuentes et al., 1988; Savoye et al., 2003).  
642 Low tide phases bringing detrital material could also cause this increase in the POC/Chl-a  
643 ratio. Another possible explanation is the dominance of zooplankton organisms that perform  
644 nocturnal vertical migration for feeding (Daro, 1988), favoring a higher POC/Chl-a ratio  
645 (heterotroph organisms; Bentaleb et al., 1998). Such explanation is supported by higher POM  
646 obtained during the nighttime, whereas the ratio was almost constant for the daytime (Table

647 S1; SI). Thus,  $Pt_{PK}$  observed during nighttime may reflect Pt levels in zooplankton organisms  
648 with two higher values at 11 pm and 1 am (2.23 and 1.85  $\mu\text{mol}\cdot\text{g}^{-1}$ , respectively). Nighttime  
649 phytoplankton cell lysis through phytoplankton grazing could result in the increasing  $Pt_D$   
650 values. As for other trace elements incorporated or adsorbed by phytoplankton, Pt might  
651 remain in the particulate phase until cell lyses and remineralization takes place (Sanders and  
652 Abbe, 1987; Sanders and Riedel, 1998).

653 The second day was more productive since much lower POC/Chl-a levels occurred (38 at  
654 11:30 am), which clearly reflect the dominance of living phytoplankton (Savoye et al., 2012).  
655 Those cells are active suggesting more intense primary production took place together with  
656 increasing solar radiation and lower SPM concentrations. Dissolved  $O_2$  saturation levels were  
657 much higher and not correlated with tide. A peak of pigment concentrations also arose at  
658 11:30 am. Interestingly, increasing  $Pt_{PK}$  concentrations occurred together with this intensified  
659 primary production. Although the degree of surface complexation with organic matter  
660 remains unknown, laboratory experiments have shown that Pt adsorption kinetics onto  
661 estuarine sediments is greatest for those with relatively high total carbon contents (Couceiro et  
662 al., 2007). The clear increase of  $Pt_{PK}$  and the evaluation of the POM as fresh living  
663 phytoplankton support the hypothesis that phytoplankton adsorb Pt. Such complexation  
664 seems more likely to take place with newly produced phytoplankton cells. This could be  
665 explained either because absorption mechanisms through the active uptake of living cells is  
666 the principal pathway or because Pt is more likely to complex and adsorb on “fresh” organic  
667 material. Concomitant increase in both,  $Pt_D$  and particulate Pt on the second day, implied an  
668 additional Pt source from upstream (i.e., end of ebb tide, Fig 2A).

#### 669 *Arcachon Bay and Genoa Harbor*

670 In the Arcachon Bay, Chl-a values were two-fold lower than in the Gironde Estuary  
671 suggesting lower productivity, probably related to the fact that this field campaign occurred in  
672 April while the one for the Gironde Estuary was in June. Lower  $O_2$  saturation levels also  
673 suggest lower production and/or higher consumption in the riverine channels of the Arcachon  
674 Bay. In fact, POC/Chl-a ratios followed the SPM variations that were tide-dependent. Ebb  
675 tides therefore brought particulate material, which can be considered as detritic or degraded  
676 plankton cells considering the rather high POC/Chl-a ratios ( $< 400$ ). Phaeopigments perfectly  
677 correlate with SPM concentrations, supporting this hypothesis. Microscopic observations  
678 during a following field campaign (Castellano M., personal communication) displayed major  
679 changes in phytoplankton composition associated to the tidal regime, suggesting that direct  
680 transport of phytoplankton (allochthonous production) and debris can play a dominant role.  
681 We also should consider the potential importance of anthropogenic POM (e.g. from urban

682 sewage; Liénart et al., 2017) in this urbanized semi-enclosed system (relatively high average  
683 POC% of 6%; Table S1, SI).

684 Since no  $Pt_{PK}$  data were available for the whole cycle in Arcachon, in contrast to the Gironde  
685 Estuary mouth, the variations in  $Pt_D$  cannot be clearly attributed to diel cycles in relation with  
686 phytoplankton production and degradation. Phytoplankton sorption might therefore not  
687 entirely explain the average  $Pt_{PK}$  concentrations of  $11.76 \pm 3.40 \text{ pmol.g}^{-1}$  of this site showing  
688 dominance of non-living organisms or detrital particulate matter. Under such conditions, one  
689 should also consider Pt complexation with inorganic particulate phases, including silt and  
690 clay, also containing Fe- and manganese-(Mn)-oxy/hydroxides, which are potentially  
691 important Pt carrier phases (Colodner et al., 1992; Jean-Soro et al., 2013; Lustig et al., 1996).  
692 The general decreasing trend in  $Pt_D$  concentrations on the second day (from 11 am to 6 pm)  
693 could yet be related to increasing primary production and subsequent Pt sequestration by  
694 phytoplankton cells.

695 In the Genoa Harbor, POC/Chl-a ratios were constant as SPM concentrations, with values  
696 below 200 suggesting the dominance of living phytoplankton. Increasing pigment  
697 concentrations featured increasing primary production during daytime that is further  
698 supported by increasing  $O_2$  saturation levels. Despite the lack of significant differences  
699 between values through time, the daytime  $Pt_D$  profile suggested an overall decreasing trend.  
700 As for the Arcachon Bay, increasing primary production and the presence of active living  
701 phytoplankton cells may have led to intensified Pt removal from the dissolved phase and  
702 subsequent algal sorption.

703

704 4.3. Platinum sorption by phytoplankton and accumulation in marine biota

705 *Transfer to phytoplankton*

706 Phytoplankton cells are efficient scavengers of trace elements, accumulating high  
707 concentrations from the surrounding medium (Sanders and Riedel, 1998). Both active and  
708 passive mechanisms can be involved in trace element sorption and the relative importance of  
709 different sorption pathways depend on the target element (Sanders and Riedel, 1998).  
710 Therefore, the observed Pt sorption by phytoplankton may reveal either: (i) active uptake of Pt  
711 by phytoplankton cells with/without relevant biological functioning (e.g., mimicking other  
712 bio-elements), (ii) passive adsorption of Pt on cell surface, or (iii) adsorption on organic  
713 ligands produced by algal cells. Extracellular production of organic ligands by phytoplankton  
714 can indeed play a major role in trace metal-organic interactions (González-Dávila, 1995). For

715 marine algae, element chemical speciation and the presence of other ions or chelators able to  
716 regulate speciation are of major importance for bioavailability (Sanders and Riedel, 1998;  
717 Sunda, 1989). Laboratory experiments showed linear increase of freshwater periphyton Pt  
718 uptake following exposure to dissolved Pt(II) and Pt(IV) (Rauch et al., 2004b). Under longer  
719 exposure time needed for Pt cellular absorption in natural environments, Pt toxicity is not  
720 excluded (Rauch et al., 2004b). Accordingly, laboratory data report that for marine algae, both  
721 adsorption and internalization are related to slow kinetics and are considerably constrained  
722 (Cosden et al., 2003; Shams et al., 2014; Turner et al., 2007). However, another study on  
723 accumulation of organic Pt species (cisplatin) by the marine macroalga *Ulva lactuca* showed  
724 greater Pt interactions at the algal surface in seawater than expected by thermodynamic or  
725 kinetic considerations (Easton et al., 2011). Considering the smaller size of marine microalgae  
726 collected through phytoplankton nets, higher surface area and therefore higher metal sorption  
727 is expected compared to sorption by macroalgae. In addition, despite their crucial importance,  
728 laboratory results obtained under controlled conditions, not considering simultaneous  
729 variations of various environmental factors affecting trace element distribution (e.g. trace  
730 metal concentrations and speciation, light, temperature, water column stability), may not be  
731 directly applicable to natural systems (Twining et al., 2011). The present study reflects, for  
732 the first time, under natural conditions, that phytoplankton might play an important role in Pt  
733 partitioning in productive coastal systems. Couceiro et al. (2007) reported that only small  
734 quantities of Pt adsorbed on POM-rich cohesive sediments is further desorbed (< 1.5 %) in  
735 chlorinated water, meaning that Pt is somewhat irreversibly adsorbed. Platinum sorption by  
736 phytoplankton could therefore control Pt budget in productive coastal zones. Such  
737 biogeochemical behavior characterizes other trace metals such as silver (Ag) for which no  
738 desorption occurs along estuarine salinity gradients when it is associated to phytoplankton  
739 (Sanders and Abbe, 1987). Silver ab- or adsorption therefore increases its retention in the  
740 estuary, reducing its transport rate. Accordingly, short-term processes including diel cycles of  
741 primary production showed their importance for other trace metals considered as biologically  
742 essential (e.g. Fe, copper: Cu, or cobalt: Co), and anthropogenic metals (e.g. lead: Pb, Pinedo-  
743 Gonzalez et al., 2014). Diel changes in such biological activity may therefore be critical for Pt  
744 cycling in coastal systems.

#### 745 *Consequences of Pt accumulation for the marine trophic chain*

746 Little information exists regarding Pt toxicity on algae. Although no significant toxicity was  
747 reported, a linear decrease of the algal photosynthetic activity in freshwater periphyton  
748 occurred under Pt exposure (Rauch et al., 2004b). Easton et al. (2011) showed no measurable  
749 reduction of efficiency in marine macroalga *U. lactuca* exposed to cisplatin in seawater. Same

750 authors predict greater uptake by *U. lactuca* when sewage effluents discharge directly Pt-  
751 based drugs into coastal waters than indirectly into fresh waters. Platinum-based complexes  
752 directly released into coastal waters are indeed more reactive than after indirect discharge  
753 allowing for estuarine mixing and the gradual conversion of these complexes back to the  
754 parent drug (Easton et al., 2011). In addition, data also report greater sorption of inorganic  
755 Pt(II) and Pt(IV) ions than cisplatin by the marine alga.

756 Phytoplankton cells are the first link in the marine trophic chain. Despite uncertainties in  
757 potential adverse effects on these cells, transfer to and accumulation in higher organisms  
758 cannot be excluded. Phytoplankton can accumulate relatively high concentrations of trace  
759 elements from their environment with BCF of up to  $10^6$  (Fisher, 1986). Few studies report  
760 environmental trace metal concentrations in algae, and therefore few BCF are available for  
761 other trace elements. The marine macroalga *U. lactuca* showed BCF of  $\sim 10^3$  to  $10^4$  for Cd,  
762 Cr, Cu, Pb, or Zn (Conti and Cecchetti, 2003). These results reflect that, with similar BCF  
763 (Table 1), Pt is as biogeochemically reactive to algae as other essential and anthropogenic  
764 trace elements of concern that have been monitored for decades in coastal environments. In  
765 wild bivalves, BCF of  $\sim 10^3$  also occurred, which are similar to levels observed in wild  
766 mussels from the Samil urban beach (Spain; Neira et al., 2015). However, in the Gironde  
767 Estuary, Cd and Ag show BCF of  $10^5$  and  $10^6$ , respectively (Lanceleur et al., 2011),  
768 suggesting that Pt uptake from seawater by bivalves is lower compared to these trace metals.

769 Since bivalve feed on algal cells, Pt uptake may also occur through the trophic pathway after  
770 phytoplankton filtration. Bivalves may also filter mineral particles included in suspended bulk  
771 material. This would be especially the case in turbid systems such as the inner Gironde  
772 Estuary. At this site, average Pt concentrations of  $3.68 \pm 1.89 \text{ pmol.g}^{-1}$  are quantified in bulk  
773 particulate material (SPM; Cobelo-García et al., 2014a) and their passage through the  
774 digestive system may contribute to Pt levels measured in bivalve tissues. Zooplankton  
775 organisms, which dominated during nighttime of Cycle 1, are also phytoplankton consumers.  
776 Assuming that  $\text{Pt}_{\text{PK}}$  concentrations measured in nighttime samples mainly originate from  
777 zooplankton organisms, lower Pt concentrations in those organisms ( $2.04 \pm 0.19 \text{ pmol.g}^{-1}$ ;  
778 Fig.2 E) and in wild oysters ( $1.69 \pm 0.15 \text{ pmol.g}^{-1}$ ; Table 1) than in phytoplankton, suggest  
779 that biomagnification of Pt concentrations did not occur at these trophic levels. These higher  
780 organisms may readily excrete Pt forms accumulated through phytoplankton consumption as  
781 observed for other trace metals (e.g. Ag, Cd; Wang and Fisher, 1998). In addition, it is  
782 possible that the dissolved phase remains the dominant uptake pathway in both bivalves and  
783 zooplankton. Accordingly, other field studies associated the absence of metal

784 biomagnification to biodilution related to higher body mass of organisms from higher trophic  
785 levels (Chernova and Lysenko, 2019; Liu et al., 2019).

786 Apart from direct feeding, sorption of Pt phytoplankton may regulate Pt forms and availability  
787 to other marine biota. Phytoplankton biotransformation may alter (enhance or reduce)  
788 contaminant toxicity to other organisms and associated adverse biological effects (Sanders  
789 and Riedel, 1998). In addition, Pt sequestration by phytoplankton cells and potential cell  
790 sinking in the water column may reduce its availability to other phytoplankton species or to  
791 higher trophic levels (e.g. Sanders and Riedel, 1998).

792

### 793 *Plankton as a biomonitor of Pt contamination*

794 In both urbanized sites, the Arcachon Bay and the Genoa Harbor,  $Pt_{PK}$  concentrations were 4  
795 to 8 times higher than in the Gironde Estuary mouth, respectively. Platinum levels in bivalves  
796 did not show such differences since they were similar in oysters from the French Atlantic  
797 coastal sites and only twice higher in mussels from the Genoa Harbor. Platinum plankton  
798 concentrations may therefore reflect the levels of anthropogenic pressure found in these three  
799 contrasting sites, with the phytoplankton from the Gironde Estuary reflecting coastal ocean  
800 conditions, whereas the Arcachon Bay and, to a greater extent, the Genoa Harbor  $Pt_{PK}$  levels  
801 feature urban/industrial human activities and associated Pt emissions. One should also  
802 consider that different plankton net mesh sizes were used in the study to retrieve plankton  
803 material for Pt analysis, i.e. 20  $\mu m$  in the Arcachon Bay and Genoa Harbor and 200  $\mu m$  in the  
804 Gironde Estuary. The analyzed plankton communities may be different in relation with the  
805 sampling, potentially biasing the  $Pt_{PK}$  comparison between sites. Moreover, if adsorption on  
806 phytoplankton cells represents an important pathway for Pt bioconcentration, the relative  
807 surface area available for Pt adsorption could have been therefore smaller in the Gironde  
808 Estuary than in the other sites due to the net mesh size. This could contribute to the lower Pt  
809 concentrations recorded in the Gironde Estuary samples. Furthermore, the relative importance  
810 of the main genera varied among the sites, as algal communities undergo species succession  
811 and changes in dominant species in different sites and seasons (Cobelo-Garcia et al. 2012).  
812 This change in the phytoplankton composition potentially induces variation in trace metal  
813 sorption. In the urbanized Arcachon Bay and the Genoa Harbor, Pt concentrations in  
814 phytoplankton were  $\sim 10$  times greater than in bivalves, whereas in the Gironde Estuary  
815 mouth there were only  $\sim$  two-fold higher (Table 1). This difference in  $Pt_{PK} / Pt_{BV}$  ratio could  
816 be related to the inner-estuary conditions of the La Fosse site, while the phytoplankton  
817 samples originated from the open coastal zone (Fig. 1A). Despite common feeding and

818 filtering mechanisms, one should also consider potential differences in trace metal uptake and  
819 accumulation that may occur between mussels and oysters, which are different bivalve species  
820 (e.g. Ruelas-Inzunza and Páez-Osuna, 2000). Sampling of the two species in the same  
821 sampling site will help to confirm our hypotheses. Higher BCF in plankton than in bivalves  
822 from the same site shows the high potentiality provided by this marine biological fraction for  
823 the monitoring of coastal metallic contamination. Given the short lifetime of phytoplankton,  
824 these cells could be a promising biomonitor for contaminant pressure at short time scales.  
825 More data would be necessary to evaluate the potential transfer of Pt from phytoplankton to  
826 different zooplankton and bivalve species. This should be done with respect to accumulation  
827 from ambient seawater as a prerequisite for reliable multi-species biomonitoring of Pt  
828 contamination, as reported in other coastal environments with different contaminants (Conti  
829 and Cecchetti, 2003). Potential irreversible Pt adsorption onto organic-rich particles (Couceiro  
830 et al., 2007) and potentially onto phytoplankton cells as previously discussed, suggest that this  
831 biological fraction could be used as tracer of Pt contamination and transport in coastal waters.  
832 More importantly, considering the rapid Pt uptake or complexation on “fresh” living  
833 phytoplankton cells (concomitant with cell production), phytoplankton could provide an early  
834 signal of Pt contamination in productive coastal systems. Phytoplankton showed great ability  
835 of accumulating this emerging contaminant several thousand times over the concentrations  
836 quantified in seawater, as other commonly used marine bioindicator species for various  
837 pollutants (e.g. Conti and Cecchetti, 2003).



## 838 **5. Conclusions and perspectives**

839 Results obtained from the three contrasting sites suggest that short-term processes, such as  
840 primary production may help understanding the marine biogeochemistry of Pt. In less  
841 urbanized sites with high primary productivity, algal Pt sorption and release appear as  
842 determinant factors in the Pt biogeochemical cycle. Through biological processes including Pt  
843 fixation by adsorption, absorption, sequestration as well as chemical biotransformation,  
844 phytoplankton can change trace metal biological reactivity and toxicity, and strongly alter Pt  
845 transport and fate. Such results are therefore valuable to shed further light on the controls of  
846 phytoplankton on the under-documented Pt reactivity in the marine environment. In contrast,  
847 in more confined and/or urbanized coastal water bodies, such biogeochemical signals may be  
848 masked by the dynamics of Pt inputs from diverse sources, such as wastewater, run off or  
849 urban aerosols. By reflecting the general state of Pt contamination of three contrasting sites  
850 comprising open coastal area and urbanized, semi-enclosed sites, and showing relatively high  
851 bioconcentration factors (up to  $10^4$ ), marine algae should be considered a relevant biomonitor  
852 of coastal short-term Pt distribution.

853 Knowing that trace metals may induce biological alterations to communities at higher trophic  
854 levels (Sanders and Riedel, 1998), there is a crucial need for more information on potential  
855 adverse effects of Pt on primary producers, i.e. the basis of the marine trophic chain. Results  
856 of this study clearly highlight the importance of considering changes occurring at hourly time-  
857 scales, when establishing sampling strategies for field campaigns on such bioreactive trace  
858 metals, as a prerequisite for obtaining representative results as already recommended in  
859 previous studies (Pinedo-Gonzalez et al., 2014). It is important to develop monitoring of Pt  
860 and other PGE in the phytoplankton fraction, including rhodium (Rh) which is predicted to  
861 participate in biological removal and transport processes in marine systems to a greater extent  
862 (Shams et al., 2014). Determination of Pt concentrations in the different functional groups and  
863 plankton classes would help understanding its cycles in the marine food chain (Twining et al.,  
864 2011). Further investigations are required in order to understand and estimate the extent of Pt  
865 sorption in phytoplankton cells, given that their potential complexation capacity could  
866 influence marine Pt cycling.

867

868 **Acknowledgements**

869 This work has benefited from the financial support of the FEDER Aquitaine-1999-Z0061, the  
870 COST Action TD1407, and the EU FP7 Ocean 2013.2 Project SCHeMA (Project-Grant  
871 Agreement 614002), which are gratefully acknowledged. Authors also gratefully  
872 acknowledge the help of the R/V Thalia Crew (TGIR FOF), the R/V Planula IV Crew (TGIR  
873 FOF), the UNIGE-It Team, the DISTAV, the R/V MASO Crew for field campaigns; A.  
874 Charrier, Dr. A. Coynel and Dr. Y. Del Amo for POC analyses, phytoplankton sampling and  
875 scientific support; A. Lerat, Dr. A. Penezić, and L. Troi for sampling and assistance during  
876 field campaigns.

877

878 **References**

- 879 Abdou, M., Schäfer, J., Gil-Díaz, T., Tercier-Waeber, M.-L., Catrouillet, C., Massa, F.,  
 880 Castellano, M., Magi, E., Povero, P., Blanc, G., 2019. Spatial variability and sources  
 881 of platinum in a contaminated harbor – tracing coastal urban inputs. *Environ. Chem.*  
 882 <https://doi.org/10.1071/EN19160>
- 883 Abdou, M., 2018. Platinum biogeochemical cycles in coastal environments. PhD thesis,  
 884 University of Bordeaux. 292pp.
- 885 Abdou, M., Dutruch, L., Schäfer, J., Zaldibar, B., Medrano, R., Izagirre, U., Gil-Díaz, T.,  
 886 Bossy, C., Catrouillet, C., Hu, R., Coynel, A., Lerat, A., Cobelo-García, A., Blanc, G.,  
 887 Soto, M., 2018. Tracing platinum accumulation kinetics in oyster *Crassostrea gigas*, a  
 888 sentinel species in coastal marine environments. *Science of The Total Environment*  
 889 615, 652–663. <https://doi.org/10.1016/j.scitotenv.2017.09.078>
- 890 Abdou, M., Schäfer, J., Cobelo-García, A., Neira, P., Petit, J.C.J., Auger, D., Chiffoleau, J.-F.,  
 891 Blanc, G., 2016. Past and present platinum contamination of a major European  
 892 fluvial–estuarine system: Insights from river sediments and estuarine oysters. *Marine*  
 893 *Chemistry*, 13th International Estuarine Biogeochemistry Symposium (IEBS) -  
 894 *Estuaries Under Anthropogenic Pressure* 185, 104–110.  
 895 <https://doi.org/10.1016/j.marchem.2016.01.006>
- 896 Abdou, M., Schäfer, J., Hu, R., Gil-Díaz, T., Garnier, C., Brach-Papa, C., Chiffoleau, J.-F.,  
 897 Charmasson, S., Giner, F., Dutruch, L., Blanc, G., 2019. Platinum in sediments and  
 898 mussels from the northwestern Mediterranean coast: Temporal and spatial aspects.  
 899 *Chemosphere* 215, 783–792. <https://doi.org/10.1016/j.chemosphere.2018.10.011>
- 900 Allen, G.P., 1971. Relationship between grain size parameter distribution and current patterns  
 901 in the Gironde estuary (France). *Journal of Sedimentary Research* 41, 74–88.  
 902 <https://doi.org/10.1306/74D721EE-2B21-11D7-8648000102C1865D>
- 903 Arnot, J.A., Gobas, F.A., 2006. A review of bioconcentration factor (BCF) and  
 904 bioaccumulation factor (BAF) assessments for organic chemicals in aquatic  
 905 organisms. *Environ. Rev.* 14, 257–297. <https://doi.org/10.1139/a06-005>
- 906 Artelt, S., Kock, H., König, H.P., Levsen, K., Rosner, G., 1999. Engine dynamometer  
 907 experiments: platinum emissions from differently aged three-way catalytic converters.  
 908 *Atmospheric Environment* 33, 3559–3567. [https://doi.org/10.1016/S1352-2310\(99\)00109-0](https://doi.org/10.1016/S1352-2310(99)00109-0)
- 910 Baudrimont, M., Schäfer, J., Marie, V., Maury-Brachet, R., Bossy, C., Boudou, A., Blanc, G.,  
 911 2005. Geochemical survey and metal bioaccumulation of three bivalve species  
 912 (*Crassostrea gigas*, *Cerastoderma edule* and *Ruditapes philippinarum*) in the Nord  
 913 Médoc salt marshes (Gironde estuary, France). *Science of The Total Environment*  
 914 337, 265–280. <https://doi.org/10.1016/j.scitotenv.2004.07.009>
- 915 Bentaleb, I., Fontugne, M., Descolas-Gros, C., Girardin, C., Mariotti, A., Pierre, C., Brunet,  
 916 C., Poisson, A., 1998. Carbon isotopic fractionation by plankton in the Southern  
 917 Indian Ocean: relationship between  $\delta^{13}\text{C}$  of particulate organic carbon and dissolved  
 918 carbon dioxide. *Journal of Marine Systems* 17, 39–58. [https://doi.org/10.1016/S0924-7963\(98\)00028-1](https://doi.org/10.1016/S0924-7963(98)00028-1)
- 920 Caetano, M., Vale, C., 2003. Trace-element Al composition of seston and plankton along the  
 921 Portuguese coast. *Acta Oecologica*, Proceedings of the Plankton Symposium, Espinho,  
 922 Portugal 24, S341–S349. [https://doi.org/10.1016/S1146-609X\(03\)00024-9](https://doi.org/10.1016/S1146-609X(03)00024-9)
- 923 Capello, M., Cutroneo, L., Ferretti, G., Gallino, S., Canepa, G., 2016. Changes in the physical  
 924 characteristics of the water column at the mouth of a torrent during an extreme rainfall  
 925 event. *Journal of Hydrology*, Flash floods, hydro-geomorphic response and risk  
 926 management 541, 146–157. <https://doi.org/10.1016/j.jhydrol.2015.12.009>

- 927 Carli, A. (Genoa U. (Italy) I. di S.A.M., Pane, L., Romairone, V., 1994. A study of  
928 phytoplankton populations of the Riva Trigoso Bay (Gulf of Genoa) in relation to  
929 eutrophication features of the water. MAP Technical Reports Series (UNEP).
- 930 Castaing, P., Allen, G.P., 1981. Mechanisms controlling seaward escape of suspended  
931 sediment from the Gironde: A macrotidal estuary in France. *Marine Geology, Estuary*  
932 *\3- Shelf Interrelationships* 40, 101–118. [https://doi.org/10.1016/0025-3227\(81\)90045-](https://doi.org/10.1016/0025-3227(81)90045-1)  
933 1
- 934 Castelle, S., Schäfer, J., Blanc, G., Dabrin, A., Lancelleur, L., Masson, M., 2009. Gaseous  
935 mercury at the air–water interface of a highly turbid estuary (Gironde Estuary,  
936 France). *Marine Chemistry, 10th International Estuarine Biogeochemistry Symposium*  
937 - “Estuaries in a Changing World” 117, 42–51.  
938 <https://doi.org/10.1016/j.marchem.2009.01.005>
- 939 Chernova, E.N., Lysenko, E.V., 2019. The content of metals in organisms of various trophic  
940 levels in freshwater and brackish lakes on the coast of the sea of Japan. *Environ Sci*  
941 *Pollut Res* 26, 20428–20438. <https://doi.org/10.1007/s11356-019-05198-8>
- 942 Cifuentes, L.A., Sharp, J.H., Fogel, M.L., 1988. Stable carbon and nitrogen isotope  
943 biogeochemistry in the Delaware estuary. *Limnology and Oceanography* 33, 1102–  
944 1115. <https://doi.org/10.4319/lo.1988.33.5.1102>
- 945 Cloern, J.E., 1996. Phytoplankton bloom dynamics in coastal ecosystems: A review with  
946 some general lessons from sustained investigation of San Francisco Bay, California.  
947 *Reviews of Geophysics* 34, 127–168. <https://doi.org/10.1029/96RG00986>
- 948 Cobelo-García, A., Bernárdez, P., Leira, M., López-Sánchez, D.E., Santos-Echeandía, J.,  
949 Prego, R., Pérez-Arlucea, M., 2012. Temporal and diel cycling of nutrients in a  
950 barrier–lagoon complex: Implications for phytoplankton abundance and composition.  
951 *Estuarine, Coastal and Shelf Science, Coastal Lagoons in a changing environment:*  
952 *understanding, evaluating and responding* 110, 69–76.  
953 <https://doi.org/10.1016/j.ecss.2012.03.015>
- 954 Cobelo-García, A., Filella, M., Croot, P., Frazzoli, C., Du Laing, G., Ospina-Alvarez, N.,  
955 Rauch, S., Salaun, P., Schäfer, J., Zimmermann, S., 2015. COST action TD1407:  
956 network on technology-critical elements (NOTICE)—from environmental processes to  
957 human health threats. *Environ Sci Pollut Res* 22, 15188–15194.  
958 <https://doi.org/10.1007/s11356-015-5221-0>
- 959 Cobelo-García, A., López-Sánchez, D.E., Almécija, C., Santos-Echeandía, J., 2013. Behavior  
960 of platinum during estuarine mixing (Pontevedra Ria, NW Iberian Peninsula). *Marine*  
961 *Chemistry* 150, 11–18. <https://doi.org/10.1016/j.marchem.2013.01.005>
- 962 Cobelo-García, A., López-Sánchez, D.E., Schäfer, J., Petit, J.C.J., Blanc, G., Turner, A.,  
963 2014a. Behavior and fluxes of Pt in the macrotidal Gironde Estuary (SW France).  
964 *Marine Chemistry, Estuarine Biogeochemistry* 167, 93–101.  
965 <https://doi.org/10.1016/j.marchem.2014.07.006>
- 966 Cobelo-García, A., Santos-Echeandía, J., López-Sánchez, D.E., Almécija, C., Omanović, D.,  
967 2014b. Improving the Voltammetric Quantification of Ill-Defined Peaks Using Second  
968 Derivative Signal Transformation: Example of the Determination of Platinum in  
969 Water and Sediments. *Anal. Chem.* 86, 2308–2313. <https://doi.org/10.1021/ac403558y>
- 970 Cobelo-García, A., Turner, A., Millward, G.E., 2008. Fractionation and Reactivity of  
971 Platinum Group Elements During Estuarine Mixing. *Environ. Sci. Technol.* 42, 1096–  
972 1101. <https://doi.org/10.1021/es0712118>
- 973 Colodner, D., 1991. The Marine Geochemistry of Rhenium, Iridium and Platinum (No.  
974 WHOI-91-30). WOODS HOLE OCEANOGRAPHIC INSTITUTION MA.
- 975 Colodner, D.C., Boyle, E.A., Edmond, J.M., 1993. Determination of rhenium and platinum in  
976 natural waters and sediments, and iridium in sediments by flow injection isotope

- 977 dilution inductively coupled plasma mass spectrometry. *Anal. Chem.* 65, 1419–1425.  
978 <https://doi.org/10.1021/ac00058a019>
- 979 Colodner, D.C., Boyle, E.A., Edmond, J.M., Thomson, J., 1992. Post-depositional mobility of  
980 platinum, iridium and rhenium in marine sediments. *Nature* 358, 402–404.  
981 <https://doi.org/10.1038/358402a0>
- 982 Conti, M.E., Cecchetti, G., 2003. A biomonitoring study: trace metals in algae and molluscs  
983 from Tyrrhenian coastal areas. *Environmental Research* 93, 99–112.  
984 [https://doi.org/10.1016/S0013-9351\(03\)00012-4](https://doi.org/10.1016/S0013-9351(03)00012-4)
- 985 Cosden, J.M., Schijf, J., Byrne, R.H., 2003. Fractionation of Platinum Group Elements in  
986 Aqueous Systems: Comparative Kinetics of Palladium and Platinum Removal from  
987 Seawater by *Ulva lactuca* L. *Environ. Sci. Technol.* 37, 555–560.  
988 <https://doi.org/10.1021/es0259234>
- 989 Couceiro, F., Turner, A., Millward, G.E., 2007. Adsorption and desorption kinetics of  
990 rhodium (III) and platinum (IV) in turbid suspensions: Potential tracers for sediment  
991 transport in estuarine flumes. *Marine Chemistry, 9th International Estuarine  
992 Biogeochemistry Symposium Estuaries and Enclosed Seas under Changing  
993 Environmental Conditions* 107, 308–318.  
994 <https://doi.org/10.1016/j.marchem.2007.02.010>
- 995 Daro, M.H., 1988. Migratory and Grazing Behavior of Copepods and Vertical Distribution of  
996 Phytoplankton [WWW Document]. URL  
997 [https://www.ingentaconnect.com/content/umrsmas/bullmar/1988/00000043/00000003](https://www.ingentaconnect.com/content/umrsmas/bullmar/1988/00000043/00000003/art00028)  
998 [/art00028](https://www.ingentaconnect.com/content/umrsmas/bullmar/1988/00000043/00000003/art00028) (accessed 9.25.19).
- 999 David, V., Sautour, B., Chardy, P., Leconte, M., 2005. Long-term changes of the zooplankton  
1000 variability in a turbid environment: The Gironde estuary (France). *Estuarine, Coastal  
1001 and Shelf Science* 64, 171–184. <https://doi.org/10.1016/j.ecss.2005.01.014>
- 1002 Djingova, R., Heidenreich, H., Kovacheva, P., Markert, B., 2003. On the determination of  
1003 platinum group elements in environmental materials by inductively coupled plasma  
1004 mass spectrometry and microwave digestion. *Analytica Chimica Acta* 489, 245–251.  
1005 [https://doi.org/10.1016/S0003-2670\(03\)00716-5](https://doi.org/10.1016/S0003-2670(03)00716-5)
- 1006 Doxaran, D., Froidefond, J.-M., Castaing, P., Babin, M., 2009. Dynamics of the turbidity  
1007 maximum zone in a macrotidal estuary (the Gironde, France): Observations from field  
1008 and MODIS satellite data. *Estuarine, Coastal and Shelf Science* 81, 321–332.  
1009 <https://doi.org/10.1016/j.ecss.2008.11.013>
- 1010 Easton, C., Turner, A., Sewell, G., 2011. An evaluation of the toxicity and bioaccumulation of  
1011 cisplatin in the marine environment using the macroalga, *Ulva lactuca*. *Environmental  
1012 Pollution* 159, 3504–3508. <https://doi.org/10.1016/j.envpol.2011.08.018>
- 1013 Essumang, D.K., 2008. Bioaccumulation of platinum group metals in dolphins, *Stenella* sp.,  
1014 caught off Ghana. *African Journal of Aquatic Science* 33, 255–259.  
1015 <https://doi.org/10.2989/AJAS.2008.33.3.8.620>
- 1016 Etcheber, H., Taillez, A., Abril, G., Garnier, J., Servais, P., Moatar, F., Commarieu, M.-V.,  
1017 2007. Particulate organic carbon in the estuarine turbidity maxima of the Gironde,  
1018 Loire and Seine estuaries: origin and lability. *Hydrobiologia* 588, 245–259.  
1019 <https://doi.org/10.1007/s10750-007-0667-9>
- 1020 Finkelman, R.B., Aruscavage, P.J., 1981. Concentration of some platinum-group metals in  
1021 coal. *International Journal of Coal Geology* 1, 95–99. [https://doi.org/10.1016/0166-5162\(81\)90006-9](https://doi.org/10.1016/0166-5162(81)90006-9)
- 1022  
1023 Fisher, N.S., 1986. On the reactivity of metals for marine phytoplankton. *Limnology and  
1024 Oceanography* 31, 443–449. <https://doi.org/10.4319/lo.1986.31.2.0443>

- 1025 Frada, M., Young, J., Cachão, M., Lino, S., Martins, A., Narciso, Á., Probert, I., Vargas, C.  
 1026 de, 2010. A guide to extant coccolithophores (Calcihaptophycidae, Haptophyta) using  
 1027 light microscopy.
- 1028 Gammons, C.H., 1996. Experimental investigations of the hydrothermal geochemistry of  
 1029 platinum and palladium: V. Equilibria between platinum metal, Pt(II), and Pt(IV)  
 1030 chloride complexes at 25 to 300°C. *Geochimica et Cosmochimica Acta* 60, 1683–  
 1031 1694. [https://doi.org/10.1016/0016-7037\(96\)00048-8](https://doi.org/10.1016/0016-7037(96)00048-8)
- 1032 Glé, C., Del Amo, Y., Bec, B., Sautour, B., Froidefond, J.-M., Gohin, F., Maurer, D., Plus,  
 1033 M., Laborde, P., Chardy, P., 2007. Typology of environmental conditions at the onset  
 1034 of winter phytoplankton blooms in a shallow macrotidal coastal ecosystem, Arcachon  
 1035 Bay (France). *J Plankton Res* 29, 999–1014. <https://doi.org/10.1093/plankt/fbm074>
- 1036 González-Dávila, M., 1995. The role of phytoplankton cells on the control of heavy metal  
 1037 concentration in seawater. *Marine Chemistry* 48, 215–236.  
 1038 [https://doi.org/10.1016/0304-4203\(94\)00045-F](https://doi.org/10.1016/0304-4203(94)00045-F)
- 1039 Goosen, N.K., Kromkamp, J., Peene, J., van Rijswijk, P., van Breugel, P., 1999. Bacterial and  
 1040 phytoplankton production in the maximum turbidity zone of three European estuaries:  
 1041 the Elbe, Westerschelde and Gironde. *Journal of Marine Systems* 22, 151–171.  
 1042 [https://doi.org/10.1016/S0924-7963\(99\)00038-X](https://doi.org/10.1016/S0924-7963(99)00038-X)
- 1043 Hasle, R., 1978. The inverted microscope method. *Phytoplankton manual* 88–96.
- 1044 Hodge, Vern., Stallard, Martha., Koide, Minoru., Goldberg, E.D., 1986. Determination of  
 1045 platinum and iridium in marine waters, sediments, and organisms. *Anal. Chem.* 58,  
 1046 616–620. <https://doi.org/10.1021/ac00294a029>
- 1047 Ifremer/ODE/LITTORAL/LERAR (2017). Qualité du Milieu Marin Littoral. Bulletin de la  
 1048 surveillance 2016. Départements: Gironde, Landes, Pyrénées Atlantiques.  
 1049 ODE/LITTORAL/LERAR/17-004. <https://archimer.ifremer.fr/doc/00388/49893/>
- 1050 Irigoien, X., Castel, J., 1997. Light Limitation and Distribution of Chlorophyll Pigments in a  
 1051 Highly Turbid Estuary: the Gironde (SW France). *Estuarine, Coastal and Shelf  
 1052 Science* 44, 507–517. <https://doi.org/10.1006/ecss.1996.0132>
- 1053 Jean-Soro, L., Oleron-Hamdous, A., Béchet, B., Legret, M., 2013. Evaluation of platinum  
 1054 distribution between different soil components. *J Soils Sediments* 13, 569–574.  
 1055 <https://doi.org/10.1007/s11368-012-0491-3>
- 1056 Kümmerer, K., Helmers, E., 1997. Hospital effluents as a source for platinum in the  
 1057 environment. *Science of The Total Environment* 193, 179–184.  
 1058 [https://doi.org/10.1016/S0048-9697\(96\)05331-4](https://doi.org/10.1016/S0048-9697(96)05331-4)
- 1059 Lanceleur, L., Schäfer, J., Chiffolleau, J.-F., Blanc, G., Auger, D., Renault, S., Baudrimont,  
 1060 M., Audry, S., 2011. Long-term records of cadmium and silver contamination in  
 1061 sediments and oysters from the Gironde fluvial–estuarine continuum – Evidence of  
 1062 changing silver sources. *Chemosphere* 85, 1299–1305.  
 1063 <https://doi.org/10.1016/j.chemosphere.2011.07.036>
- 1064 Lenz, K., Koellensperger, G., Hann, S., Weissenbacher, N., Mahnik, S.N., Fuerhacker, M.,  
 1065 2007. Fate of cancerostatic platinum compounds in biological wastewater treatment of  
 1066 hospital effluents. *Chemosphere* 69, 1765–1774.  
 1067 <https://doi.org/10.1016/j.chemosphere.2007.05.062>
- 1068 Liénart, C., Savoye, N., Bozec, Y., Breton, E., Conan, P., David, V., Feunteun, E., Grangeré,  
 1069 K., Kerhervé, P., Lebreton, B., Lefebvre, S., L’Helguen, S., Mousseau, L., Raimbault,  
 1070 P., Richard, P., Riera, P., Sauriau, P.-G., Schaal, G., Aubert, F., Aubin, S., Bichon, S.,  
 1071 Boinet, C., Bourasseau, L., Bréret, M., Caparros, J., Cariou, T., Charlier, K., Claquin,  
 1072 P., Cornille, V., Corre, A.-M., Costes, L., Crispi, O., Crouvoisier, M., Czamanski, M.,  
 1073 Del Amo, Y., Derriennic, H., Dindinaud, F., Durozier, M., Hanquiez, V., Nowaczyk,  
 1074 A., Devesa, J., Ferreira, S., Fournier, M., Garcia, F., Garcia, N., Geslin, S., Grossteffan,

1075 E., Gueux, A., Guillaudeau, J., Guillou, G., Joly, O., Lachaussée, N., Lafont, M.,  
1076 Lamoureux, J., Lecuyer, E., Lehodey, J.-P., Lemeille, D., Leroux, C., Macé, E., Maria,  
1077 E., Pineau, P., Petit, F., Pujo-Pay, M., Rimelin-Maury, P., Sultan, E., 2017. Dynamics  
1078 of particulate organic matter composition in coastal systems: A spatio-temporal study  
1079 at multi-systems scale. *Progress in Oceanography* 156, 221–239.  
1080 <https://doi.org/10.1016/j.pcean.2017.03.001>

1081 Liu, J., Cao, L., Dou, S., 2019. Trophic transfer, biomagnification and risk assessments of  
1082 four common heavy metals in the food web of Laizhou Bay, the Bohai Sea. *Science of  
1083 The Total Environment* 670, 508–522. <https://doi.org/10.1016/j.scitotenv.2019.03.140>

1084 López-Sánchez, D.E., Cobelo-García, A., Rijkenberg, M.J.A., Gerringa, L.J.A., de Baar,  
1085 H.J.W., 2019. New insights on the dissolved platinum behavior in the Atlantic Ocean.  
1086 *Chemical Geology* 511, 204–211. <https://doi.org/10.1016/j.chemgeo.2019.01.003>

1087 Luoma, S.N., Geen, A. van, Lee, B.-G., Cloern, J.E., 1998. Metal uptake by phytoplankton  
1088 during a bloom in South San Francisco Bay: Implications for metal cycling in  
1089 estuaries. *Limnology and Oceanography* 43, 1007–1016.  
1090 <https://doi.org/10.4319/lo.1998.43.5.1007>

1091 Lustig, S., Zang, S., Michalke, B., Schramel, P., Beck, W., 1996. Transformation behaviour of  
1092 different platinum compounds in a clay-like humic soil: speciation investigations.  
1093 *Science of The Total Environment* 188, 195–204. [https://doi.org/10.1016/0048-  
1094 9697\(96\)05172-8](https://doi.org/10.1016/0048-9697(96)05172-8)

1095 Mashio, A.S., Obata, H., Gamo, T., 2017. Dissolved Platinum Concentrations in Coastal  
1096 Seawater: Boso to Sanriku Areas, Japan. *Arch Environ Contam Toxicol* 73, 240–246.  
1097 <https://doi.org/10.1007/s00244-017-0373-1>

1098 Mashio, A.S., Obata, H., Tazoe, H., Tsutsumi, M., Ferrer i Santos, A., Gamo, T., 2016.  
1099 Dissolved platinum in rainwater, river water and seawater around Tokyo Bay and  
1100 Otsuchi Bay in Japan. *Estuarine, Coastal and Shelf Science* 180, 160–167.  
1101 <https://doi.org/10.1016/j.ecss.2016.07.002>

1102 Neira, P., Cobelo-García, A., Besada, V., Santos-Echeandía, J., Bellas, J., 2015. Evidence of  
1103 increased anthropogenic emissions of platinum: Time-series analysis of mussels  
1104 (1991–2011) of an urban beach. *Science of The Total Environment* 514, 366–370.  
1105 <https://doi.org/10.1016/j.scitotenv.2015.02.016>

1106 Nygren, Olle., Vaughan, G.T., Florence, T.Mark., Morrison, G.M.P., Warner, I.M., Dale,  
1107 L.S., 1990. Determination of platinum in blood by adsorptive voltammetry. *Anal.  
1108 Chem.* 62, 1637–1640. <https://doi.org/10.1021/ac00214a020>

1109 Obata, H., Yoshida, T., Ogawa, H., 2006. Determination of picomolar levels of platinum in  
1110 estuarine waters: A comparison of cathodic stripping voltammetry and isotope  
1111 dilution-inductively coupled plasma mass spectrometry. *Analytica Chimica Acta* 580,  
1112 32–38. <https://doi.org/10.1016/j.aca.2006.07.044>

1113 Pađan, J., Marcinek, S., Cindrić, A.-M., Layglon, N., Garnier, C., Salaün, P., Cobelo-García,  
1114 A., Omanović, D., 2019. Determination of sub-picomolar levels of platinum in the  
1115 pristine Krka River estuary (Croatia) using improved voltammetric methodology.  
1116 *Environ. Chem.* <https://doi.org/10.1071/EN19157>

1117 Peavy, C.C., 1958. The Importance of Platinum in Petroleum Refining [WWW Document].  
1118 URL  
1119 [https://www.ingentaconnect.com/content/matthey/pmr/1958/00000002/00000002/art0  
1120 0003](https://www.ingentaconnect.com/content/matthey/pmr/1958/00000002/00000002/art00003) (accessed 9.26.19).

1121 Petit, J.C.J., Schäfer, J., Coynel, A., Blanc, G., Deycard, V.N., Derriennic, H., Lancelleur, L.,  
1122 Dutruch, L., Bossy, C., Mattielli, N., 2013. Anthropogenic sources and  
1123 biogeochemical reactivity of particulate and dissolved Cu isotopes in the turbidity

- 1124 gradient of the Garonne River (France). *Chemical Geology* 359, 125–135.  
 1125 <https://doi.org/10.1016/j.chemgeo.2013.09.019>
- 1126 Pinedo-Gonzalez, P., West, A.J., Rivera-Duarte, I., Sañudo-Wilhelmy, S.A., 2014. Diel  
 1127 Changes in Trace Metal Concentration and Distribution in Coastal Waters: Catalina  
 1128 Island As a Study Case. *Environ. Sci. Technol.* 48, 7730–7737.  
 1129 <https://doi.org/10.1021/es5019515>
- 1130 Platt, T., Sathyendranath, S., Ulloa, O., Harrison, W.G., Hoepffner, N., Goes, J., 1992.  
 1131 Nutrient control of phytoplankton photosynthesis in the Western North Atlantic.  
 1132 *Nature* 356, 229–231. <https://doi.org/10.1038/356229a0>
- 1133 Rauch, S., Hemond, H.F., Peucker-Ehrenbrink, B., 2004a. Recent Changes in Platinum Group  
 1134 Element Concentrations and Osmium Isotopic Composition in Sediments from an  
 1135 Urban Lake. *Environ. Sci. Technol.* 38, 396–402. <https://doi.org/10.1021/es0347686>
- 1136 Rauch, S., Paulsson, M., Wilewska, M., Blanck, H., Morrison, G.M., 2004b. Short-Term  
 1137 Toxicity and Binding of Platinum to Freshwater Periphyton Communities. *Arch  
 1138 Environ Contam Toxicol* 47, 290–296. <https://doi.org/10.1007/s00244-004-3197-8>
- 1139 REPHY – French Observation And Monitoring Program For Phytoplankton And Hydrology  
 1140 In Coastal Waters, 2019. REPHY dataset - French Observation and Monitoring  
 1141 program for Phytoplankton and Hydrology in coastal waters. 1987-2018 Metropolitan  
 1142 data. <https://doi.org/10.17882/47248>
- 1143 Ruchter, N., Zimmermann, S., Sures, B., 2015. Field Studies on PGE in Aquatic Ecosystems,  
 1144 in: Zereini, F., Wiseman, C.L.S. (Eds.), *Platinum Metals in the Environment*,  
 1145 *Environmental Science and Engineering*. Springer Berlin Heidelberg, Berlin,  
 1146 Heidelberg, pp. 351–360. [https://doi.org/10.1007/978-3-662-44559-4\\_22](https://doi.org/10.1007/978-3-662-44559-4_22)
- 1147 Rudnick, R.L., Gao, S., 2003. Composition of the Continental Crust. *Treatise on  
 1148 Geochemistry* 3, 659. <https://doi.org/10.1016/B0-08-043751-6/03016-4>
- 1149 Ruelas-Inzunza, J.R., Páez-Osuna, F., 2000. Comparative bioavailability of trace metals using  
 1150 three filter-feeder organisms in a subtropical coastal environment (Southeast Gulf of  
 1151 California). *Environmental Pollution* 107, 437–444. [https://doi.org/10.1016/S0269-7491\(99\)00157-8](https://doi.org/10.1016/S0269-7491(99)00157-8)
- 1153 Ruggieri, N., Castellano, M., Capello, M., Maggi, S., Povero, P., 2011. Seasonal and spatial  
 1154 variability of water quality parameters in the Port of Genoa, Italy, from 2000 to 2007.  
 1155 *Marine Pollution Bulletin* 62, 340–349.  
 1156 <https://doi.org/10.1016/j.marpolbul.2010.10.006>
- 1157 Sanders, J.G., Abbe, G.R., 1987. The role of suspended sediments and phytoplankton in the  
 1158 partitioning and transport of silver in estuaries. *Continental Shelf Research, Dynamics  
 1159 of Turbid Coastal Environments* 7, 1357–1361. [https://doi.org/10.1016/0278-4343\(87\)90040-9](https://doi.org/10.1016/0278-4343(87)90040-9)
- 1161 Sanders, J.G., Riedel, G.F., 1998. Metal accumulation and impacts in phytoplankton, in:  
 1162 Langston, W.J., Bebianno, M.J. (Eds.), *Metal Metabolism in Aquatic Environments*.  
 1163 Springer US, Boston, MA, pp. 59–76. [https://doi.org/10.1007/978-1-4757-2761-6\\_4](https://doi.org/10.1007/978-1-4757-2761-6_4)
- 1164 Savoye, N., Aminot, A., Tréguer, P., Fontugne, M., Naudet, N., Kérouel, R., 2003. Dynamics  
 1165 of particulate organic matter  $\delta^{15}\text{N}$  and  $\delta^{13}\text{C}$  during spring phytoplankton blooms in a  
 1166 macrotidal ecosystem (Bay of Seine, France). *Marine Ecology Progress Series* 255,  
 1167 27–41. <https://doi.org/10.3354/meps255027>
- 1168 Savoye, N., David, V., Morisseau, F., Etcheber, H., Abril, G., Billy, I., Charlier, K., Oggian,  
 1169 G., Derriennic, H., Sautour, B., 2012. Origin and composition of particulate organic  
 1170 matter in a macrotidal turbid estuary: The Gironde Estuary, France. *Estuarine, Coastal  
 1171 and Shelf Science, ECSA 46 Conference Proceedings* 108, 16–28.  
 1172 <https://doi.org/10.1016/j.ecss.2011.12.005>



- 1173 Schäfer, J., Hannker, D., Eckhardt, J.-D., Stüben, D., 1998. Uptake of traffic-related heavy  
1174 metals and platinum group elements (PGE) by plants. *Science of The Total*  
1175 *Environment* 215, 59–67. [https://doi.org/10.1016/S0048-9697\(98\)00115-6](https://doi.org/10.1016/S0048-9697(98)00115-6)
- 1176 Sen, I.S., Peucker-Ehrenbrink, B., 2012. Anthropogenic disturbance of element cycles at the  
1177 Earth's surface. *Environ. Sci. Technol.* 46, 8601–8609.  
1178 <https://doi.org/10.1021/es301261x>
- 1179 Shams, L., Turner, A., Millward, G.E., Brown, M.T., 2014. Extra- and intra-cellular  
1180 accumulation of platinum group elements by the marine microalga, *Chlorella*  
1181 *stigmatophora*. *Water Research* 50, 432–440.  
1182 <https://doi.org/10.1016/j.watres.2013.10.055>
- 1183 Sottolichio, A., Castaing, P., 1999. A synthesis on seasonal dynamics of highly-concentrated  
1184 structures in the Gironde estuary. *Comptes Rendus de l'Académie des Sciences -*  
1185 *Series IIA - Earth and Planetary Science* 329, 795–800. [https://doi.org/10.1016/S1251-](https://doi.org/10.1016/S1251-8050(00)88634-6)  
1186 [8050\(00\)88634-6](https://doi.org/10.1016/S1251-8050(00)88634-6)
- 1187 Strady, E., Blanc, G., Baudrimont, M., Schäfer, J., Robert, S., Lafon, V., 2011. Roles of  
1188 regional hydrodynamic and trophic contamination in cadmium bioaccumulation by  
1189 Pacific oysters in the Marennes-Oléron Bay (France). *Chemosphere* 84, 80–90.  
1190 <https://doi.org/10.1016/j.chemosphere.2011.02.051>
- 1191 Strickland, J.D.H., Parsons, T.R., 1972. A practical handbook of seawater analysis. Fisheries  
1192 Research Board of Canada.
- 1193 Sunda, W.G., 1989. Trace Metal Interactions with Marine Phytoplankton. *Biological*  
1194 *Oceanography* 6, 411–442. <https://doi.org/10.1080/01965581.1988.10749543>
- 1195 Suzuki, A., Obata, H., Okubo, A., Gamo, T., 2014. Precise determination of dissolved  
1196 platinum in seawater of the Japan Sea, Sea of Okhotsk and western North Pacific  
1197 Ocean. *Marine Chemistry* 166, 114–121.  
1198 <https://doi.org/10.1016/j.marchem.2014.10.003>
- 1199 Turner, A., 2007. Particle–water interactions of platinum group elements under estuarine  
1200 conditions. *Marine Chemistry* 103, 103–111.  
1201 <https://doi.org/10.1016/j.marchem.2006.08.002>
- 1202 Turner, A., Lewis, M.S., Shams, L., Brown, M.T., 2007. Uptake of platinum group elements  
1203 by the marine macroalga, *Ulva lactuca*. *Marine Chemistry* 105, 271–280.  
1204 <https://doi.org/10.1016/j.marchem.2007.02.009>
- 1205 Twining, B.S., Baines, S.B., 2013. The Trace Metal Composition of Marine Phytoplankton.  
1206 *Annual Review of Marine Science* 5, 191–215. [https://doi.org/10.1146/annurev-](https://doi.org/10.1146/annurev-marine-121211-172322)  
1207 [marine-121211-172322](https://doi.org/10.1146/annurev-marine-121211-172322)
- 1208 Twining, B.S., Baines, S.B., Bozard, J.B., Vogt, S., Walker, E.A., Nelson, D.M., 2011. Metal  
1209 quotas of plankton in the equatorial Pacific Ocean. *Deep Sea Research Part II: Topical*  
1210 *Studies in Oceanography, Plankton Dynamics and Carbon Cycling in the Equatorial*  
1211 *Pacific* 58, 325–341. <https://doi.org/10.1016/j.dsr2.2010.08.018>
- 1212 United Nations, 2017. Factsheet: People and Oceans. The Ocean Conference, New York, 5-9  
1213 June 2017.
- 1214 Utermöhl, H., 1958. Methods of collecting plankton for various purposes are discussed. *SIL*  
1215 *Communications*, 1953-1996, 9, 1–38.  
1216 <https://doi.org/10.1080/05384680.1958.11904091>
- 1217 Vyas, N., Turner, A., Sewell, G., 2014. Platinum-based anticancer drugs in waste waters of a  
1218 major UK hospital and predicted concentrations in recipient surface waters. *Science of*  
1219 *The Total Environment* 493, 324–329. <https://doi.org/10.1016/j.scitotenv.2014.05.127>
- 1220 Wang, W.-X., Fisher, N.S., 1998. Excretion of trace elements by marine copepods and their  
1221 bioavailability to diatoms [WWW Document].  
1222 <https://doi.org/info:doi/10.1357/002224098765213649>

1223 Zingone, A., Totti, C., Sarno, D., Cabrini, M., Caroppo, C., Giacobbe, M.G., Luglio, A.,  
1224 Nuccio, C., Socal, G., 2010. Fitoplancton: metodiche di analisi quali-quantitativa.  
1225 Manuali e Linee Guida 56/2010 213–237.  
1226